Title
Optimization of Albedo for Human Thermal Comfort

Author
Khan, Rafiur Rahman

Publication Date
2023

Peer reviewed|Thesis/dissertation

Optimization Of Albedo For Human Thermal Comfort

By

RAFIUR RAHMAN KHAN

THESIS

Submitted in partial satisfaction of the requirements for the degree of

MASTER OF SCIENCE

in

Civil and Environmental Engineering

in the

OFFICE OF GRADUATE STUDIES

of the

UNIVERSITY OF CALIFORNIA

DAVIS

Approved:

Dr. John T. Harvey, UC Davis, Chair

Dr. Hui Li, Tongji University

Dr. Somayeh Nassiri, UC Davis

Committee in Charge

2023

Rafiur Rahman Khan
Master's Thesis, March. 2023
Advisor: Dr. John Harvey
Civil and Environmental Engineering
University of California Davis

Optimization of Albedo for Human Thermal Comfort

Abstract

In the context of urban microclimates, thermal comfort serves as the key indicator to describe people's subjective impression of temperature in open spaces. It gives a general review of how the sun, wind, air temperature, and humidity affect the ability to perceive heat. But nowadays human thermal comfort is being compromised due to the urban heat island effect. The phenomenon known as the urban heat island (UHI) occurs when the temperature in metropolitan regions is higher than in the nearby rural areas. Urban heat islands are a source of growing concern since they can have an impact on communities by worsening air pollution and greenhouse gas emissions (due to increased air conditioner use), increasing the likelihood of heat-related disease, and possibly even raising mortality rates. For this purpose, evaluating the human thermal comfort level would be a significant step in adapting feasible solutions to reduce the adverse effect of the urban heat island. The goal of this study is to simulate the microclimate using the ENVImet (V4) computer and the RayMan model to increase albedo, or the ratio of reflected incoming radiation, for the human thermal comfort index. The ENVImet (V4) software is validated using air temperature and solar radiation data gathered in several USA locations. The microclimate simulator ENVImet can be used to determine the high-resolution geographical and temporal distribution of microclimate variables within an urban region .The RayMan model was created for the physiological equivalent temperature measurement and the estimation of the mean radiation temperature along with thermal indices in simple and complex situations .

Historical information about places with changeable seasonal circumstances was used for simulation and analysis after the necessary inputs and limits for the models are determined. The results of the simulation was used to assess the level of thermal comfort for both adults and children and recommendations would be provided to improve human thermal comfort.

The study conducted on microclimate simulation of four scenarios of asphalt and concrete pavement using Envimet and optimization with Rayman has led to the conclusion that an optimal albedo value of 0.15 is ideal. Although the study was conducted based on data from two months, June and July, further research can improve the accuracy of the findings. The results of this study are valuable as they provide insights into the effects of different pavement types on the microclimate and can help in the design and planning of sustainable urban environments. It is essential to consider the impact of pavements on the microclimate and the resulting effects on the urban ecosystem, especially in the context of global warming and climate change.

Acknowledgments

This thesis assignment requires work on my part. but, it would not have been possible without the kind support and help of many individuals. I want to start by expressing my sincere gratitude to Prof. John Harvey, who served as my advisor, for giving me the chance to pursue my study on the optimization of albedo for human thermal comfort and for his ongoing support, encouragement, and guidance throughout the research process. His guidance helped me to conduct the study in the proper manner. I also want to thank the other members of my committee, Associate Professor Somayeh Nassiri and Professor Hui Li, for their support, wisdom, and insightful criticism of this thesis. I would also like to express my gratitude to Dr. Ali A. Butt for his mentorship and advice during the development of my thesis. Finally, and maybe most importantly, I want to thank my family and friends for their unwavering compassion, inspiration, support, and assistance throughout my life.

List of Abbreviations

Abbreviations	Definitions
Chapter 1	
CO	Carbon Dioxide
NO	Nitric Oxide
PM	Particulate Matter
SO	Sulfur Dioxide
UHI	Urban Heat Island
VOCs	Volatile Organic Compound
Chapter 2	
GHG	Green House Gas
PMV	Predicted Mean Vote
PT	Perceived Temperature
OT	Operative Temperature
SET	Standard Effective Temperature
MRT	Mean Radiant Temperature
VMT	Vehicle Miles Travel
PET	Physiological Equivalent Temperature

TABLE OF CONTENTS

Abstract ii
Acknowledgments iv
List of abbreviations v
Table of contents vi
List of Tables xii
List of Figures xiv

Chapter 1 Introduction 1
1.1 Heat island effect 2
1.2 Potential effects on heat islands 4
1.2.1 Impact on human comfort and health 4
1.2.2 Increased Energy Use 5
1.2.3 Emissions of Air pollutants and Green House Gases 6
1.2.4 Impact on Pavement Life 6
1.3 Albedo and the necessity of its optimization for human thermal comfort 7

Chapter 2 Literature Review 8
2.0 Methodology of Literature Survey 8
2.1 Albedo and human thermal comfort 9
2.2 Thermal Comfort Index 10
2.3 Different studies 11
2.3.1 Study 1: Impact of albedo in heatwave conditions in London 11
2.3.2 Study 2: Influence on albedo 15
2.4 Summary of research and knowledge gaps 18
2.4.1 Environmental Performance 18
2.4.2 Implementation issues 19

Chapter 3: **Problem Statement and Study Methodologies** 20
3.1 Problem statement 20
3.2 Study goal and scope 21
3.3 Method 21
3.4 Study Objectives 22
3.5 Tasks 22
3.6 Organization of the following parts of this thesis 23

Chapter 4: Simulation 24
4.1 Introduction 24
4.1.2. Pavement Surface Details 24
4.1.3 Pavement Thermal and other Properties 24
4.2 Different limits of human thermal comfort: General Concepts 26
4.3 Thermal comfort index 31
4.4 General Pavement Parameters 40

4.5 Models Followed by Envimet and Rayman Software 42
4.6. Envimet Simulation 43
4.7 Sample Simulation 50
4.8. Sample result of Envimet 50
4.9 Use of Simulation results 50

Chapter 5 Analysis and Findings: Optimization of Albedo on Human Thermal Comfort 52
5.1 The Rayman Model 52
5.1.1 Input Details 52
5.2 Optimization of albedo 54
5.3 Optimization Setup in Rayman 57
5.4 Findings of the optimization 58
5.5 Limitations of optimization 59
5.6 Recommendations of optimization 60
5.7 Discussions of optimization 60
5.8 Correlation Analysis 61
5.9 Wind speed and correlation. 61
5.10 Overall results from Envimet and Rayman. 69
5.11 Study questions and answers 70
5.12 Study limitations 71

Chapter 6: Summary, Conclusions and Recommendations

6.1 Summary and Conclusions 72
6.2 Recommendations and possible application of the study 73
List of Tables
List of Figures
Appendix

LIST OF TABLES

Table 2.1: Envimet base model material reflectivity and coefficients 12
Table 2.2 Envimet scenarios tested 12
Table 2.3 Variation of albedo 14
Table 4.1. Metabolic rates at different activities 36
Table 4.2. Thermal sensation classifications for different regions. 39
Table 4.3 to 4.10 Input details for Envimet 46-49
Table 4.11 Sample Simulation Results 50
Table 5.1 to 5.4 Input details for Rayman 52-54
Table 5.5 to 5.6 Albedo optimization 57
Table 5.7 to 5.12 Correlation Analysis 65-68

LIST OF FIGURES

Figure 1.1: Urban heat island (UHI) effect 3
Figure 1.2: Example of electrical load versus air temperature for New Orleans, LA 5
Figure 2.1: A Study of heatwave conditions in London 11
Figure 2.2: The measured incoming and reflected radiation 13
Figure 2.3 Methodology Workflow 15
Figure 2.4 Analysis Outdoor and courtyard monitored air temperature 17
Figure 4.0: Predicted Mean vote and Predicted Percentage of Dissatisfaction 26
Figure 4.1 Illustration of heat budget on the human body 33
Figure 4.2. Illustration of energy balance model on human body 38
Figure 4. 3 to 4.6 Input scenarios for Envimet 44-45
Figure:4.7 Interaction between Envimet and Rayman 51
Figure 5.1 to 5.3 Simulation Input 52-53
Figure 5.4 to 5.5 Predicted percentage of dissatisfaction vs Albedo 58-59
Figure 5.6 to 5.11 Surface Temperature v Albedo 60-62

Chapter 1 Introduction

The urban heat island (UHI) is a phenomenon whereby temperature levels in urban areas are higher than in surrounding rural settings. Urban heat islands are a matter of increasing concern since they can affect communities by exacerbating air pollution and greenhouse gas emissions.The use of air conditioning is increasing which contributes to the increase of global warming. And there is also the occurrence of heat-related illness,that may lead to higher levels of mortality (1). There will probably be more heat waves in many places as a result of the summer heat load brought on by climate change, and they'll probably last longer and be more intense (1).

Urban heat islands depend not only on the character of physical processes but also on urban planning approaches (2). There exists a strong relationship between the UHI effect and urban configuration (3). The wind and thermal regimes of the cities depend on the land cover and land-use character of the urban territory (4).Urban heat island effect reduction can be achieved because of increased evapotranspiration: as the vegetation cover releases latent heat and at the same time reduces the amount of energy available for heating, green areas can potentially cool the surrounding area (5). The natural process of tree transpiration lowers the temperature (6).The green cover of vegetation also reduces the intensity of direct solar exposure and helps to transfer the received solar radiation into latent heat. Water bodies are another feature that can help to reduce thermal load due to a transpiration effect and higher specific heat (7). The heat island effect can also be reduced by decreasing anthropogenic heat (8).

The environmental implications connected to each stage of the life cycle of various civil infrastructures are receiving more and more attention. Roadways and pavements, as a significant component of the built environment and the transportation infrastructure system, are essential to the advancement of society and the economy. Researchers, organizations, businesses, and other stakeholders in the field of

roads and pavements are collaborating to lessen the environmental implications of these structures while fostering economic and social development.

One environmental impact that pavements can help reduce is the heat island effect, which is considerable due to the local climate and urban density (6).

1.1 **Heat Island Effect:**

UHI is a phenomenon when urban areas experience higher temperatures compared to their surrounding non-urban areas (9). The adverse effect of UHI has been widely documented in the literature. For example, it increases the temperature of cities; contributes to global warming (10); initiates storms/precipitation events (11); increases the energy demand of cities (12); and contributes to heat-related mortality (13). These devastating effects necessitate devising ways to mitigate the UHI effects (14). As a result, it is critical to know what factors cause the UHI effect, so that these factors can be targeted to lessen the effect through appropriate policy interventions (15).

Studies have derived the UHI effect in three ways depending on their measurement altitudes: boundary UHI, canopy UHI and surface UHI (16). Boundary UHI is measured from the altitude of the rooftop to the atmosphere (17). It is generally used to investigate the UHI effect at mesoscale (i.e., 1–10,000 km^2) and is derived using, radiosondes (18). Canopy UHI is measured at the altitude that ranges from the ground surface to the rooftop (18). An assessment of canopy UHI is most suitable for a microscale study and is generally derived based on weather station data (19). Surface/ skin UHI (SUHI) is measured at the earth's surface level. Researchers often used satellite images (e.g., thermal bands of Landsat TM/ETM/ OLI) to derive the surface UHI effect. It is measured by calculating the difference in land surface temperature (LST) between urban/built-up and non-urban areas (e.g., waterbody and vegetation areas). NASA (20) defined LST as "how hot the surface of the Earth would feel to the touch in a particular location". Further information about LST is available on 'Comprehensive Remote Sensing' Textbook (21).

The urban heat island (UHI) effect is widely recognized as a heat accumulation phenomenon, which is the most obvious characteristic of urban climate caused by urban construction and human activities.

In the early 19th century, scholar Lake Howard first measured and discussed UHI effect when studying urban climate in London, England. Since then, many scholars around the world conducted deep research on the characteristics of UHI effect reaching that UHI effect has close relationship with urban heat release, properties and structure of underlying surface, vegetation coverage, population density and weather conditions. Meanwhile, the scale and intensity of UHI effect will be increasingly serious with the on-going urbanization. It is studied that UHI effect of Szeged(Hungary) and New York are 3.1°C and 8.0°C respectively. Meanwhile, it is found that China is also experiencing severe UHI effect in many modern cities, especially the average temperature difference on the outskirt of Beijing reaches 3.3°C from 1961 to 2000, and UHI effect of Shanghai reaches 7.4°C. Urban temperature, especially surface temperature, is the energy balance center of urban surface and one of the most important factors affecting urban climate, regulating, and controlling various ecological processes(2).

Urbanization has become increasingly intensive, leading to a constant rise in surface temperature and altering the flow of urban resources and energy. More importantly, the structure and function of the urban ecological system will also be changed, affecting urban residents health.

Source: World Meteorological Organization

Figure 1.1: Urban heat island (UHI) effect

In addition, the UHI effect (**Figure 1.1)** has received great attention from urban meteorologists. But, due to the complexity of the research object, little research on ecological and environmental effects caused by the UHI effect has been so far conducted from the perspective of the ecosystem (2). So, in this context, assessing Human Thermal Comfort is a major factor.

Many studies have been conducted to understand the urban thermal climate or the potential for heat island mitigation using this framework of simplified algorithms. In more recent efforts, researchers have incorporated more sophisticated parameterization schemes that have included distributions of demography, policies, and behavior of government; ecological variables and ecosystem services; land use and land cover change patterns; and social and economic factors to represent the complicated effects of UHI (22).

1.2 **Potential effects of heat island:**

The benefits of the heat island's wintertime warming are recognized in colder cities at higher latitudes and/or elevations. Summertime cool spots in urban locations can be created by high-rise buildings' surrounding shade. But the consequences of the summer heat island are viewed as a problem in most cities, particularly high-density cities (6). The talk that follows is centered on areas with scorching summers and wet winters.Urban heat islands' elevated temperatures can have an impact on a community's environment and quality of life, especially in the summer. While the effects of heat islands, such as extending the growing season for plants and requiring less heating energy in cold locations, appear to be favorable, the majority are negative, as noted below:

1.2.1 **Impact on human comfort and health:**

By causing general discomfort, respiratory issues, heat cramps and exhaustion, non-fatal heat stroke, and heat-related mortality, higher air pollution levels, increased daytime pavement and near-surface air temperatures, reduced nighttime cooling, and associated conditions can have an adverse effect on

human health. The effects of heat wave, which are periods of extremely hot and frequently humid weather, can also be exacerbated by heat islands. Children, older people, and people with preexisting medical disorders are sensitive populations that are particularly at risk from these incidents. Extremely risky and associated with a higher risk of untimely death, excessive heat episodes or sudden and sharp temperature spikes could result in above-average mortality rates.

The discomfort brought on by the pavement's heat stress will likely deter people from walking or bicycling, which will lessen the possibility that they will choose to travel short distances by walking or biking rather than by driving and would also influence their health. This will harm efforts to develop a community that is sustainable, livable, and walkable. So, ensuring Human thermal comfort has been a challenge now a days (23).

1.2.2 **Increased Energy Use:**

Summertime temperatures in cities may result in an increase in the amount of energy needed to cool buildings in hotter climates (e.g., Figure 1.4).

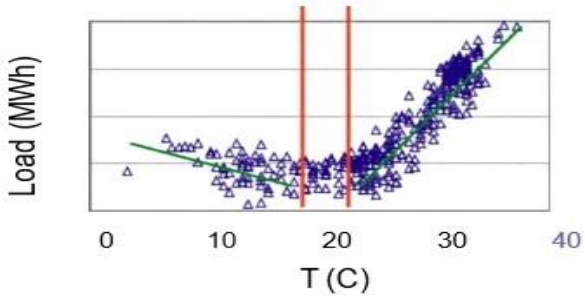

Figure 1.2. Example of electrical load versus air temperature for New Orleans, LA(24).

Figure 1.2 shows that electricity demand for building cooling increases 1.5–2.0% for every 1°F (0.6°C) increase in air temperatures, starting from 68–77°F (20–25°C). This finding implies that 5–10% of the

community's overall electricity demand is used to offset the heat island effect. In addition, the findings suggested that to increase energy consumption for cooling buildings, long periods of parking or driving on hot pavement may result in increased energy demand for cooling automobiles (23,24).

1.2.3 **Emissions of Air Pollutants and Green House Gases:**

Urban heat islands, as before mentioned, increase summertime electrical energy consumption. Electricity providers often rely heavily on fossil fuel power plants to service a large portion of this demand, especially in China and India. As a result, air pollution and greenhouse gas emissions rise. Sulfur dioxide (SO), nitrogen oxides (NO), particulate matter (PM), carbon monoxide (CO), and mercury (Hg) are the main pollutants produced by fossil fuel power plants (25,26). In addition to being dangerous to human health, these pollutants have a role in complicated air quality issues such the production of ground-level ozone (smog), fine particulate matter, and acid rain. Carbon dioxide (CO), a greenhouse gas that contributes to global climate change, is one of the greenhouse gases whose emissions are increased by the increased use of fossil fuel-powered plants.Elevated temperatures can directly accelerate the pace of ground-level ozone production in addition to their effect on energy-related emissions. NO and volatile organic compounds (VOCs) combine in the presence of sunlight and warm weather and thus ground-level ozone is created (27).

1.2.4 **Impact on pavement life:**

The temperature of the pavement can have a significant impact on how long it lasts. If asphalt pavements in tropical climates are not properly built, high summer temperatures can considerably increase the risk of rutting (permanent deformation), aging, and cracking (28, 29). The likelihood of thermal stress-induced cracking in concrete pavements can be greatly increased by high temperatures and temperature gradients (30, 31). The effects of temperature on pavement durability, however, vary depending on the type of pavement. Furthermore, it's still unclear exactly how certain pavements, including permeable pavements, would be affected.

As a result of reducing thermal deteriorations, such as rutting and/or cracking caused by the pavement's temperature and temperature gradient, cool pavements and related cooling technologies may increase the pavement's durability.

Cities must adapt to this phenomenon, prioritizing the improvement of outdoor environmental quality. Urban materials have a significant impact on outdoor environment quality, energy demand, citizens' well-being, and human thermal comfort. Optimizing the albedo (ratio of reflected radiation to incoming radiation) might lead to improving human thermal comfort.

1.3 **Albedo and the necessity of its optimization for human thermal comfort**

Albedo is the measurement of the reflectivity of sunlight by any object (32). Objects reflecting more sunlight have high albedo while those reflecting less have a low albedo. It is measured on a scale of 0–1 or given in percentage, with 1 being a perfect reflector (100%) and 0 (0%) absorbing all incoming light (33).Since the variation of solar radiation might affect human thermal comfort and can cause thermal distress, it is important to optimize albedo for achieving the desired human thermal comfort.

Chapter 2 Literature Review

2.0 Methodology of literature survey:

The literature survey is a critical aspect of any study that seeks to investigate a specific research question. It is critical to provide a thorough understanding of the research area, including the current state of knowledge, research gaps, and potential avenues for further research. It also helps to ensure that the study is based on a solid foundation of existing knowledge and can lead to more robust research findings.

The methodology of the literature survey involves a systematic and comprehensive search for relevant literature to identify existing research gaps and establish a foundation for the study. In this study, the literature search was conducted using keywords such as 'Albedo,' 'Optimization,' 'Urban Heat Island, 'Human Thermal Comfort', 'Scientific Study' etc. These keywords were used to identify relevant scientific papers that addressed the research problem. The primary source of scientific papers used in this literature survey were journal articles, books, and chapter of books. The literature survey involved a comprehensive review of relevant literature, which included both theoretical and empirical studies, to provide a broad understanding of the research area. The literature search was conducted using several electronic databases, including Google Scholar, Web of Science, and Scopus, to ensure that all relevant literature was identified. The literature survey provided the foundation for the study and helped to ensure that the research question was adequately addressed.

2.1 **Albedo and human thermal comfort:**

The study's primary goal is to simulate microclimates in order to optimize albedo for human thermal comfort. People will experience a heated environment in the summer, especially in tropical climates. When outside of a range of maximal human comfort, in structures, and in vehicles, this contributes to general discomfort on streets and parking lots (if air conditioning is not being used). In addition, discomfort from the heat, heat-related illnesses such heat exhaustion, heat cramps, and non-fatal heat stroke may also develop. The thermal discomfort could be lessened by concentrating on human thermal comfort.The reduced pavement surface and near-surface air temperature could help improve thermal comfort without increasing cooling-energy demand.

In addition, improved human thermal comfort could potentially encourage more outdoor activities (34), including potentially more walking and cycling over driving for short-distance trips. Thus improving thermal comfort will help to improve the quality of life.

The effectiveness of high-albedo materials at improving outdoor thermal comfort is currently being studied, and the findings may vary depending on the urban layout and latitude (2) (Ie., solar angle). Numerous research suggested that enhancing road reflectivity would reduce the intensity of UHI and improve outdoor thermal comfort (35). The usage of highly reflecting materials, on the other hand, has been shown in the studies to potentially have a detrimental effect on summertime thermal comfort (36). However, very limited studies were found that assess the effects of optimization of albedo measures on improving human thermal comfort. So, comprehensive models should be used to assess the optimization of albedo pertinent to the thermal environment and thermal comfort indices.

2.2 **Thermal comfort index:** Thermal comfort is influenced by many factors, such as the surrounding thermal environment (temperature, humidity, radiation flux, air flow), human activities, clothing, and perception of how hot an area is.

Assessing comfort outdoors is not simple due to the complexity and methodological differences observed in the related literature, which make any comparison with available results difficult. Generally, comfort can be assessed by means of comfort indices. There are many different indices referred to in the literature, such as Predicted Mean Vote (PMV), Perceived Temperature (PT), Operative Temperature (OP), Standard Effective Temperature (SET), Mean Radiant Temperature (MRT), Physiological Equivalent Temperature (PET) (e.g. 39-54).

But most of these indices have been developed from and for uniform indoor thermal environments, mostly using a single factor, and therefore might not be suitable for spatially and temporally severely non-uniform outdoor thermal environments. Hence, a rational index that combines several significant factors (e.g., temperature, humidity, radiation flux, air flow, etc.) into a single variable, which sums up their simultaneous effects on the sensory and physiological responses of the body, should be identified and chosen for the assessment of outdoor thermal comfort.

Moreover, considerable variability exists in the tolerance levels of different people (with age, health, and gender being the of the variables (54). Consequently, criteria for the thermal comfort index also need to be based on the form of population mean or on the tolerance levels of more sensitive members of the population. One research paper by Ahmed (55) presents findings on defining outdoor comfort based on field investigations conducted in Dhaka, Bangladesh, a city in the tropics. Findings from a survey conducted on many randomly selected people from urban spaces are presented. The findings include factors affecting comfort outdoors for Dhaka and a comfort regime based on environmental limits for urban outdoors.

2.3 **Different studies related to albedo and human thermal comfort:**

To understand the impact of albedo on thermal climate, the studies are being discussed below.

2.3.1 Study 1: Impact of albedo in heatwave conditions in London (37):

Location and methodology:

This study was based on microclimate simulations using the software ENVImet (V4.4.3), validated with air temperature and solar radiation data measured in a residential area of London. ENVI-met is a microclimate simulator able to calculate the high-resolution spatial and temporal distribution of microclimate variables within an urban domain.

a) Radiation measurement points in three roads (K_Rd, S_Rd and L_Rd); b) albedometer and radiation measuring at eaves level; c) installation of the temperature sensor on the lamppost; d) cherry picker,used for radiation measurements. (37)

Figure 2.1: A Study of heatwave conditions in London

Process:

An air temperature sensor was installed in a radiation screen at 5m height on a lamppost in the case study area (**Figure 2.1** c).

A Bluetooth temperature, humidity, and dew point sensor beacon and data logger were used with a temperature resolution of 0.1ºC and accuracy of 0.3ºC, with a greatest 0.4ºC at -10ºC to +75ºC. Spot measurements of the incoming and reflected solar radiation in different points within the canyons of the study area were performed on the 23rd of May 2019 under clear sky conditions (**Figure** 2.1 a, ,2.1b and 2.1d).An albedometer composed of two pyranometer pointing one upward and the other one downward was used to measure the incoming radiation from the upper hemisphere and the reflected radiation from the lower hemisphere at three levels within canyons: at the street level (1.2m height), at the 2nd-floor level (5m height) and at the eaves level (10m height).

Analysis:

An ENVImet model of the area was built to simulate the microclimate and thermal comfort implications of changing the reflectance of roads and facades in the case study area. A base model (Table 2.1) corresponding to the current situation was built based on field surveys, GIS data and satellite data (Google Earth) for urban geometry and vegetation.

Material & reflectivity coefficients		K_rd		S_Rd		L_Rd	
Façade (divided by orientation)		ESE	WNW	SSW	NNE	SSE	NNW
Red Bricks	r= 0.32	9%	40%		69%	8%	4%
Yellow bricks	r= 0.43	25%		33%		31%	33%
painted brick	r= 0.2	9%					
Dark paints	r= 0.08			3%	1%		
White painted bricks	r= 0.56	38%	35%	40%	17%	33%	42%
Clear glass	r= 0.05	19%	25%	24%	13%	28%	22%
Roads							
Tarmac	r= 0.19	100%		100%		100%	

Table 2.1: Envimet base model material reflectivity and coefficients (37)

Scenarios	A1 - High reflectivity facades	A2 - Low reflectivity facades	A3 - High reflectivity Roads	A4 – Combined scenario
Facades	r = 0.6	r = 0.1	as base case	r = 0.1
Roads	as base case	as base case	r = 0.5	r = 0.5

Table 2.2: Envimet scenarios evaluated (37)

A survey of materials was conducted to estimate the reflectivity and emissivity properties of facades, paving and road materials to be used in the ENVImet model. Some scenarios were simulated, changing the surface albedo of facades and roads as reported in table 2.4. The surface albedo values for the scenarios “high reflective facades” and “high reflective roads” were set to 0.6 and 0.5 respectively; these are common values found in the scientific literature on high albedo materials for microclimate mitigation.

Results:

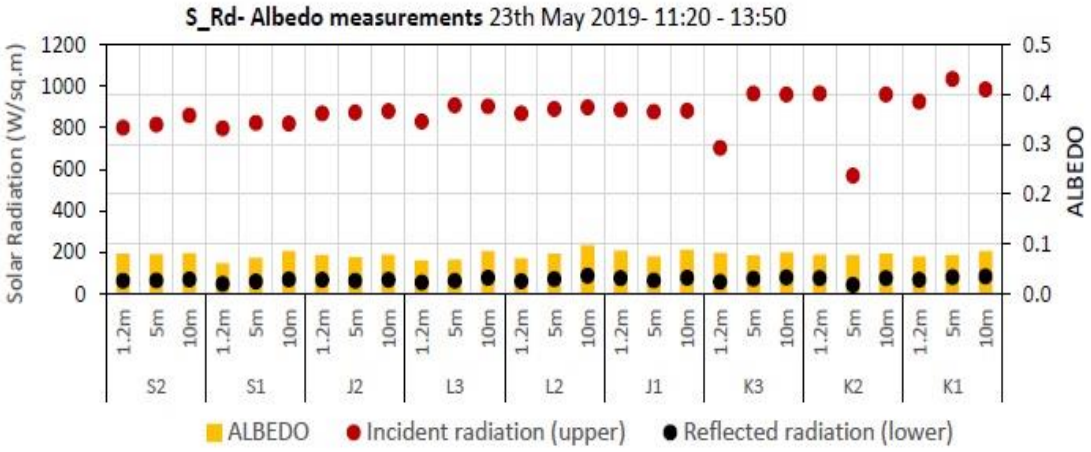

Figure 2.2: The measured incoming and reflected radiation within the three case-study urban canyons. (37) In **Figure 2.2,** The three canyons have the same geometry ratio (i.e., ratio of the building heights to the street width) of approximately 0.75 and different orientations and material distribution as reported in table 2.1 .

Table 2.3: Variations of albedo:

Location	Urban Albedo Variation
1.Street level	06-.09(Average.08)
2.second floor	the greatest and minimum values of 0.08 and 0.07 and an average value of 0.08.
3.Eaves level	The UA varied between 0.1 and 0.08, with an average value of 0.09.
4. Point L2	The highest values of UA (0.1) were recorded at point L2, namely in the street with the façade that received more radiation at the time of measurements (South-Southeast oriented façade).

Findings:

In the first study, the researchers discussed that increasing the surface albedo of urban materials may have countering effects on urban microclimate and outdoor thermal comfort. On the one hand, increasing the albedo of surfaces determines a decrease in surface temperatures. On the other hand, the consequent increase of reflections within complex urban geometry leads to an increase in solar radiation received by urban surfaces, which may have a negative impact on outdoor and indoor thermal comfort.

In terms of air temperature, changing the albedo of facades does not influence the air temperature. A significant decrease in air temperature is instead obtained with the increase in road albedo (scenario A3). On the other hand, for the studied geometry, increasing the reflectivity of facades (scenario A1) has a negligible impact also on the mean radiant temperature. Conversely, a substantial decrease in facade albedo (scenario A2) allows a reduction of the mean radiant temperature at the street level.

2.3.2 **Study 2: Influence on albedo under Mediterranean hot summer climate conditions** (38):

The study uses simulation results to evaluate the impact of different surface albedo on the thermal performance and comfort of a courtyard in Seville. To do so, the simulation tool ENVImet, one of the most widely used for outdoor spaces, is validated through a comparison with monitoring results.

Based on the monitoring and simulation stages, the study recommends the best albedo configuration for a specific courtyard condition in terms of thermal performance and user comfort, as well as a set of recommendations for consideration when designing this kind of space.

Methodology:

To achieve the aim of this study, the methodology followed comprises both monitoring and simulation. stages**(Figure 2.3).** Two different monitoring campaigns were performed in this courtyard, in two stages of the configuration of the courtyard. The subsequent simulation stage of the methodology also had two parts. The monitored data was used to validate the software to then simulate greater albedo modifications in the courtyard.

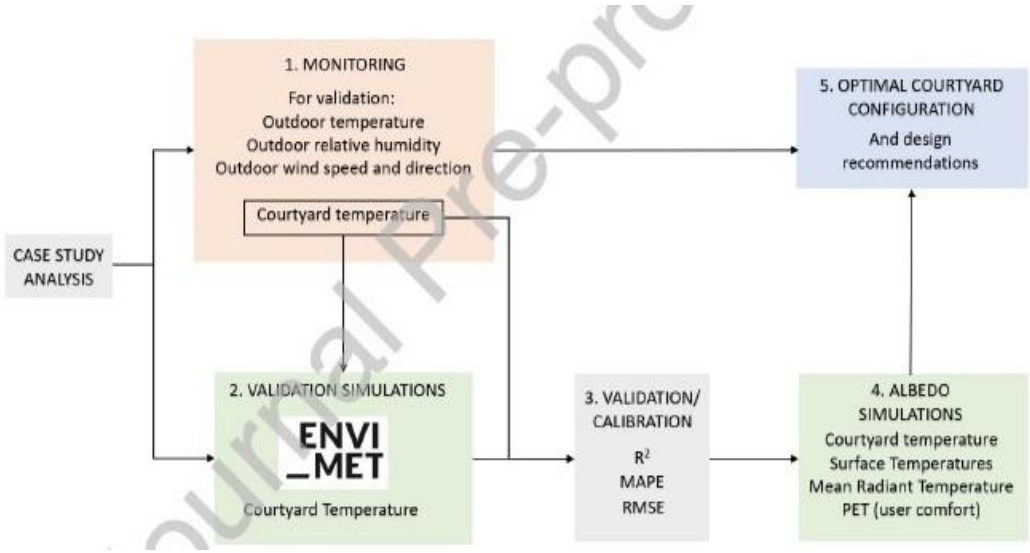

Figure 2.3: Methodology Workflow (38)

Location:

The case study selected was the courtyard of an educational building in Seville, in the south of Spain. The case study selected is the only inner courtyard in the building, built in 1976 and refurbished in 2017. The courtyard's main modifications were the enlargement of windows, the white coating added to the walls, and the floor covered with white gravel instead of soil with vegetation. A green facade was later installed on the southwest wall.

Process:

The first monitoring campaign was developed in October 2017, after the building refurbishment and at once before the installation of the green facade. The second, in August 2018, was carried out after the installation of the green facade in the courtyard. Both campaigns were over a weeklong and the building was unoccupied to limit external variables due to users. The data used for the validation of the simulation software were one day chosen for Test 1 (T1) from the first campaign and one day for Test 2 (T2) from the second. The campaigns were developed during warm days of the year when temperatures close to 38 °C were reached. This is common in August (summer) but was an anomaly for this year to reach those temperatures in October (autumn).

Simulation:

ENVImet v4.4.5, one of the most widely used Computational Fluid Dynamics (CFD) software for urban microclimate simulations on a global scale, has been used for the simulation.

The simulation process had two stages (**Figure 2.4**). First, a given day was selected from each monitoring campaign for the comparison of monitoring and simulation data in different scenarios to confirm and calibrate the software. Once it was validated, it was used to analyze different albedo configurations to set up the optimal design for the courtyard.

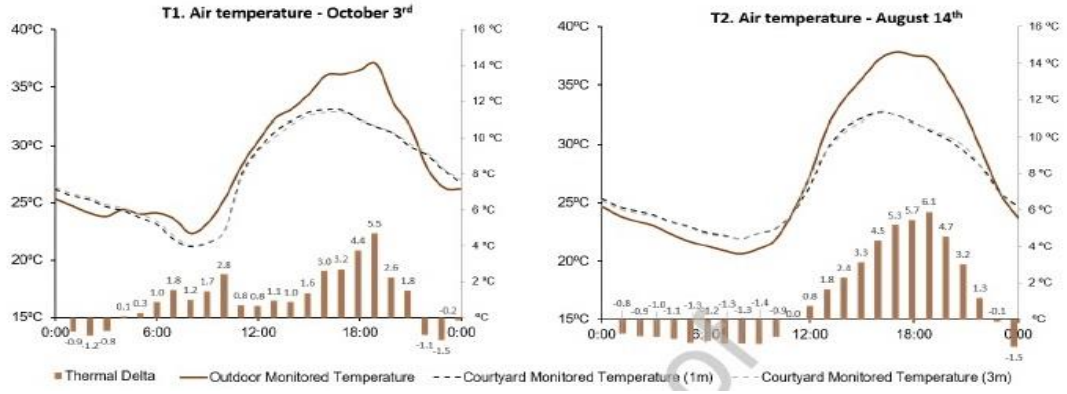

Figure 2.4: Analysis of Outdoor and courtyard monitored air temperature. Left: October 3, 2017 (without green facade). Right: August 14, 2018. (With green facade). (38)

Findings:

Two aspects relating to these results were further analyzed. The first of these is the shift between the peak temperature outside and inside the courtyard. While the greatest temperature inside the courtyard appears when the sun is at its zenith, outdoors, the greatest temperature is reached a few hours later. Inside the courtyard, the temperature peaks when the highest solar radiation is hitting the walls and floor. After this point, the courtyard geometry results in a decrease in solar radiation, and it starts cooling. Outdoors, the heat continues to accumulate after the zenith time, so that in the exterior the peak temperature is reached later. The second aspect is the relative increase in outdoor temperature observed at night in October. This causes the courtyard temperature, which is generally higher than nighttime outdoor temperatures (because of the heat absorbed by the walls), to fall below the outdoor temperature.

Key results

- Albedo played a minor role in air temperature and a larger role in MRT and PET. But, the MRT and PET value results obtained in this study remain quite high and would still cause a person to suffer from strong heat stress inside the courtyard.

- Walls with high albedo reflect solar radiation, affecting user comfort, while a low albedo on the walls absorbs radiation and increases surface temperature and air temperature. Although the recommendations on albedo helped to increase comfort, they are not enough to reach comfort in extreme conditions. To achieve comfort, the researchers concluded that the strategy of selecting an adequate albedo must be combined with other strategies such as the use of shading or evaporative cooling, especially in this kind of low Aspect Ratio courtyard.

2.4 Summary of research and knowledge gaps

Although the amount of research work has been completed or is being conducted by different research institutes and groups around the world, there are still several knowledge gaps related to the albedo optimization technique, as well as human thermal comfort level concepts for different scenarios. Some major research and knowledge gaps are identified from the literature review above and summarized as follows:

2.4.1 **Environmental Performance**

(1) Studies related to the impact of the albedo of different materials on human thermal comfort are still very low.

(2) Studies related to fundamental material properties (thermal property) of pavement, such as albedo, thermal conductivity, and heat capacity, are very limited.

(3) The seasonal effects on the local microclimate of pavements have not been fully investigated, especially the variable effects in different seasons under different climate conditions.

(4) The relationship between Mean Radiant Temperature, Physiological Equivalent Temperature, and albedo is lacking in the investigation.

2.4.2 **Implementation issues**

(1) Comprehensive recommendations for implementation and further research on human thermal comfort are missing.

(2) Use of software and the latest updated technologies have been implemented very little practically to perform comparative analysis.

Chapter 3 Problem Statement and Study Methodologies

3.1 Problem statement

This study was based on microclimate simulation through the software ENVImet (V4) and RayMan modelling software for the purpose of optimizing albedo. ENVImet (V4) software is validated with air temperature and solar radiation data measured in different areas of the USA. ENVImet is a microclimate simulator able to calculate the high-resolution spatial and temporal distribution of microclimate variables within an urban domain (56). In the context of urban microclimates, thermal comfort is the key indicator to describe people′s subjective experience of temperature in open spaces. It summarizes the impact of sun, wind, air temperature, and humidity on thermal sensation. Thus, a simulation software Envimet and Human body energy balance model will be used to calculate the thermal comfort. The RayMan model, developed for the calculation of the mean radiation temperature and thermal indices in simple and complex environments, is only based on data of air temperature, air humidity and wind speed (57). RayMan can be used for the assessment of urban bio climate and thermal indices such as Predicted Mean Vote (PMV), Physiologically Equivalent Temperature (PET) and Standard Effective Temperature (SET). The model is developed based on the German VDI-Guidelines 3789, Part II(58): Environmental Meteorology, Interactions between Atmosphere and Surfaces; Calculation of the short- and long wave radiation and VDI-3787(59): Environmental Meteorology, Methods for the human-bio meteorological evaluation of climate and air quality for the urban and regional planning at the regional level. Part I: Climate(60).The detailed calculation for thermal comfort and human energy fluxes is based on the Munich Energy Balance Model (MEMI)for Individuals**.**

3.2 **Study goal and scope**

After identifying the required inputs and limits for the models, historical data of specific locations were used from weather websites. Data were used for analysis and calculation by considering Adult Human Thermal Comfort Index for both Adults and Children. Finally, albedo was optimized for the human thermal comfort index.

3.3 **Methods:**

Environmental limits, Human Thermal Comfort inputs, and relevant inputs and limits required for the models were identified first, following the selection of experimental data that were used for the models. A Different thermodynamic model in ENVIMET allowed a holistic evaluation of steady-state and transient thermal comfort conditions.

The human thermal comfort index and PET were calculated using the RayMan model. MRT (Mean Radiant Temperature) (61) were used to calculate the net heat gain. The human body energy balance model (61,62) was used to calculate the energy gain or losses. The total energy gains or losses of a human body were calculated by the energy balance equation. The equations played an important role in calculating the value of PET. Simulation and Analysis were computed through EnviMET and RayMan. Next, Rayman was used for optimizing the albedo through 'additional pre-setting option'.

The questions to be answered by the study are:

(i)Can the EnviMet model give the desired result/output that can be used for albedo optimization?

(ii)Can EnviMet/RayMan allow albedo to be changed?

(iii)Can Envi-Met/RayMan predict the pavement temperature and other microclimate factors?

(iv)Can Envimet & RayMan measure and evaluate the human thermal comfort level for adults and children?

(v)Can I know the height that is required from/for PET (physiological equivalent temperature) model?

(vi)Is there an optimum albedo, or does it monotonically affect human thermal comfort ?

3.4 **Study objectives:**

To achieve the study goal above, the specific research objectives are listed as follows:

(i)Use of historical data and conducting microclimate-based simulation.

(ii)Using the outputs for optimizing albedo to get a value indicating better human thermal comfort.

For human thermal comfort, adults (35 years) and children (3-9 years) were considered.

Types of different built environment scenarios: Playground/Parking lot like the flat area: Asphalt and Concrete Pavement.

3.5 **Tasks:**

1. A literature review was conducted

2. Background study was performed.

3.Historical data collection was performed.

4. A situational analysis were undertaken with the inclusion of the field notes, relevant data, and inputs.

5. Data was analysed, and Results were collected.

6. A research report was written that combined the understanding of the relevant theory and previous research with the results of the current research.

7. Finally recommendations/findings were provided, and possible implementation possibilities based on future needs were given.

3.6 **Organization of the following parts of this Thesis:**

This thesis is organized as follows. Chapter 4 presents the simulation technique. Chapter 5 will discuss the optimization technique of albedo for human thermal comfort. While chapter 6 will give the summary, conclusions, and recommendations.

Chapter 4: Simulation

4.1 Introduction:

Pavement heat can influence near-surface air temperature profiles and consequently influence human thermal comfort and air quality in recent periods. Besides the thermal impact on near-surface air, pavement heat can potentially affect the temperatures of the surrounding surfaces as well as produce reflection of solar radiation and albedo that can be absorbed by surrounding surfaces, consequently affecting human thermal comfort.

The objective of the study presented in this chapter was to understand the basic process of conducting microclimate analysis and to evaluate human thermal comfort through the simulation process.

4.1.2. Pavement Surface Details: Asphalt and concrete(hardscape) pavement surface (flat areas like a parking lot, and playgrounds) was considered for the simulation.

4.1.3 Pavement Thermal and other Properties: There are important properties of pavement that are significant for the study as well as for performing the simulation.

Heat Capacity:

Heat Capacity is the energy needed to raise a unit mass of a substance by one unit of temperature, typically expressed in units of J/kg•K. The heat capacity of dense-graded asphalt and concrete are very similar, being about 900 J/kg•K which was also considered for the simulation purpose as the default value. (63).For the analysis, the value of heat capacity and thermal conductivity were kept constant for both asphalt and concrete conditions with the standard values mentioned above.

Thermal Conductivity:

Thermal conductivity is a measure of the ability of a material to conduct or transmit heat. It is the ratio of heat flux (power per unit area) to temperature gradient, and is expressed in units of W/m•K. A material with a high thermal conductivity will transfer heat at a higher rate than a material having a low thermal conductivity. The thermal conductivity of pavement in the reported literature was mentioned as 2.0 W/m•K, for asphalt and concrete. (42).The same value was also considered as default value for the simulation in Envimet and Rayman.

Albedo: It is the measurement of the reflectivity of sunlight by any object (64). Objects reflecting more sunlight have high albedo while those reflecting less have a low albedo. It is measured on a scale of 0–1 or given in percentage with 1 being a perfect reflector (100%) and 0 (0%) absorbing all incoming light (33).An albedo of 0 means no reflecting power on a perfectly black surface, while an albedo of 100% means perfect reflection of an entirely white surface. There are different albedos at different light wavelengths, and that albedo measured with an albedometer is the sum of all of those. The simulation would be conducted to measure the values of Albedo and to optimize it.

Physiological Equivalent Temperature(PET): It is defined as the physiological equivalent temperature at any given place (outdoors or indoors) and is equivalent to the air temperature at which, in a typical indoor setting, the heat balance of the human body (work metabolism 80 W of light activity, added to basic metabolism; heat resistance of clothing 0.9 clo) is maintained with core and skin temperatures equal to those under the conditions being assessed (65). Clo is a value that describes the degree of insulation provided by an article of clothing. The simulation would also calculate PET which would be a great indicator of human thermal comfort.

Mean Radiant Temperature (MRT): It is defined as the uniform temperature of an imaginary enclosure (or environment) in which the radiant heat transfer from the human body is equal to the radiant heat transfer in the actual nonuniform enclosure (or environment) (66**).** MRT was also used to assess human thermal comfort and can be calculated through simulation.

Predicted Mean Vote (PMV): It is an index that aims to predict the mean value of votes of a group of occupants on a seven-point thermal sensation scale. (67). PMV is an important factor that would be required to compare human thermal comfort with the other values calculated from the simulation.

The predicted percentage of dissatisfaction (PPD) index: Provides an estimate of how many occupants in a space would feel dissatisfied by the thermal conditions.

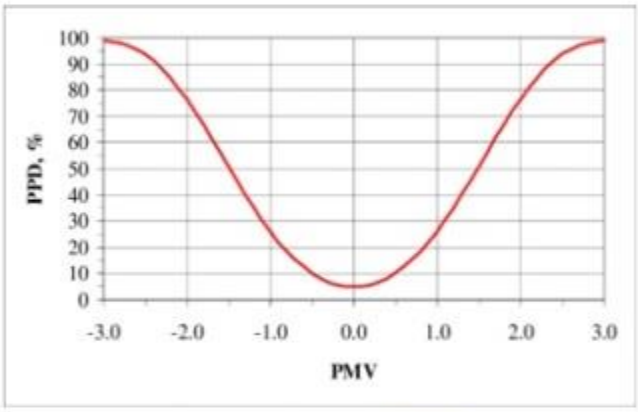

PPD as a function of PMV (Source)

Figure 4.0: **Predicted Mean vote and Predicted Percentage of Dissatisfaction**

Source: The American Society of heating, refrigerating and air-conditioning engineers(ASHRAE) (67)

4.2 Different limits of human thermal comfort: General Concepts

Although there are many factors that are related to human thermal comfort, not every factor can be discussed due to study limitations. Some of the significant factors are discussed below:

4.2.1 Importance of Mean Radiant temperature (MRT) on human thermal comfort model:

MRT is the most important parameter governing human energy balance, especially on hot sunny days. MRT also has a powerful influence on thermos physiological comfort indexes such as physiological equivalent temperature (PET) or predicted mean vote (PMV) ((61,62).

Difference between MRT and air temperature

Radiant heat can play a significant role in achieving thermal comfort, promoting a healthier environment, and lowering building heating costs in winter. To understand how radiant heat makes these benefits possible we must first clarify the difference between ambient air temperature as opposed to the mean radiant temperature. The ambient air temperature is a measure of the average air temperature in the environment while the mean radiant temperature is a measure of the net radiant heat gain and heat loss in the environment.

Most people are familiar with how fluctuations in air temperature affect their perception of comfort, but relatively few people are conscious of how their comfort is affected by mean radiant temperature differences. Living human skin has extraordinarily high emissivity and absorptivity, making it very sensitive to radiant heat loss and gain. Radiant heat loss or gain is not dependent on the air temperature. For example, when you stand in the sun on a cold winter day you feel radiant heat gained from the sun even though the air temperature is cold. On the other hand, when you open the freezer door on a hot summer day you feel radiant heat loss to the interior of the freezer. In both cases, thermal comfort is largely affected by the difference in radiant heat gain or loss, not air temperature.

Further, it is important to understand that one can experience heat gain from a warm surface and heat loss from an icy surface at the same time from different parts of the body. In other words, one's skin can simultaneously absorb heat from a warm surface and emit heat to an icy surface.

Depending on the strength of the radiation of heat from the warm surface to someone's skin and the absorption or heat from someone's skin to the icy surface, he will feel either a net gain or loss of heat energy. The mean radiant temperature measures this combined net radiant heat loss and gain (61,62).

4.2.2 Calculation of MRT in the human thermal comfort model:

To calculate the MRT *(Tmrt,* in °C), the relevant properties and dimensions of the radiating surfaces and the sky view factors as well as the posture of the human body (e.g., seated or standing, etc.) need to be known. The entire surroundings of the human body are divided into ri thermal surfaces with the temperatures *T,* (in °C) and emissivity c,, to which the view factors N, are to be assigned as weighting factors (i=l,2,3, ...,n) (61,62).

$$T_{mrt} = \left[\frac{1}{\sigma} \sum_{i=1}^{n} (E_i + \alpha_{hb} \frac{D_i}{\varepsilon_{hb}}) VF_i + F_{hb} \alpha_{hb} \frac{SVF_{hb} I}{\sigma \varepsilon_{hb}} \right]^{0.25} - 273 \quad (4.1)$$

αhb is the absorptivity of the human body surface for the short-wave radiation (standard value 0.7); *εhb* is the emissivity of the human body surface (standard value 0.97); *SVFhb* is the sky view factor of the human body. *Fhb* is the human body surface projection factor, which is a function of the incident radiation direction and the body posture. For practical application in human biometeorology, it is generally sufficient to determine *Fhb* for a rotationally symmetric person standing up or walking. *Fhb* ranges from 0.308 for 0° of the solar angles and 0.082 for 90°(50,51) where, *E;* is the emitted long-wave radiation from each surface, which can be calculated as (σ is the Stefan-Boltzmann constant, 5.67 • 10 ' W/m^2K^4):

$$E_i = \varepsilon_i \sigma (T_i + 273)^4 \quad (4.2)$$

$$D_i = (1 - \alpha_i) SVF_i I \quad (4.3)$$

Di is the diffuse short-wave radiation from each surface, mainly the diffusely reflected global. radiation. It can be calculated through equation 4.3 (*I* is the total global radiation; *SVFi* is the sky view factor of surface *i*; *αi* is the absorptivity of the surface *i* for the short-wave radiation.).

Sky View Factor can be calculated using Rayman Modelling Software by providing the albedo input. For this purpose, fish eye images of pavements are generally used in RayMan software. The fisheye images equidistantly follow linear transects to cover a range of SVF values and to analyze the reaction of the methods to a continuously changing environment (68).The "Sky View Factor" (SVF) gauges how much sky is visible from a certain location. One would have a 100% sky view factor if they could see a whole half dome of sky in an infinite plane. A portion of the sky is obscured as soon as something is placed on the infinite plane, such as trees, buildings, or hills.

More details associated with determining the view factors N; are discussed in ASHRAE literature(67). In the case of large flat surfaces without any restriction of the horizon, for instance, a larger paved parking lot, the problem of determining VF; is reduced to an upper and a lower hemisphere with a view factor of 0.5 for each (61,62).

Some important Thermal Comfort Factors based on ASHRAE:

(i)Airspeed:

The rate of air movement at a given point in time regardless of the direction.

(ii)**Clothing insulation factor:** Clo is a value that describes the degree of insulation provided by an article of clothing.The unit used to represent thermal insulation from clothing, where 1clo = winter clothing and 0.5 clo = summer clothing. There is a difference between clothing insulation (Icl), which includes even parts of the occupants' body uncovered by clothing, and garment insulation (Iclu), which only refers to heat transfer obtained from skin to clothing contact.

(iii)Metabolic Rate (M):

The rate of transformation of chemical energy into heat and mechanical work by metabolic activities within an organism, usually expressed in terms of unit area of the total body surface. In this standard, the metabolic rate is expressed in met units. This unit is accounted for as the personal activity of occupants, where one met is a person at rest.

(iv)Relative Humidity (RH):

The ratio of the partial pressure (or density) of the water vapor in the air to the saturation pressure (or density) of water vapor at the same temperature and the same total pressure.

(v)Mean Radiant Temperature (tr):

The uniform surface temperature of an enclosure where an occupant would exchange the same amount of heat as in the actual non-uniform space, calculated from the weighted temperature average of each surface divided by the total area of the space.

4.2.3 Thermal comfort index:

Generally, thermal comfort is influenced by many factors, such as the surrounding thermal environment (temperature, humidity, radiation flux, air flow, etc.), people's activity, clothing, perception of how hot an area is, etc. Assessing comfort outdoors is not simple due to the complexity and methodological differences observed in the related literature, which make any comparison with available results difficult. Generally, comfort can be assessed by means of comfort indices. There are a large number of different indices referred to in the literature, such as Predicted Mean Vote (PMV), Index of Thermal Stress (ITS), Perceived Temperature (PT), Operative Temperature (OP), Mean Radiant Temperature (MRT), Standard Effective Temperature (SET), and Physiological Equivalent Temperature (PET) (69-71).

Compared to other thermal comfort index such as ITS, PT and OP, which are more suitable for the indoor thermal environments, the SET and PET are more rational for evaluating the outdoor thermal environments. Both SET and PET are based on the human body energy balance, which use a two-node model (skin and core nodes) to model the thermal conditions of the human body physiologically relevantly. Both SET and PET are defined as the air temperature at which, in a typical indoor setting, the heat budget of the human body is balanced with the same core and skin temperatures as under the complex outdoor conditions to be evaluated. To better understand these two indices, the human body energy balance modeling should be first introduced and understood.

4.2.4 Human body energy balance modeling

The heat exchange between the human body and the thermal environment is illustrated in Figure 4.1**.** The total energy gains or losses of the human body can be described by the heat balance equation (61,62):

$$M + W + C + R + E_{sw} + C_{res} + E_{res} = S \qquad (4.4)$$

M is the metabolic rate (W/m^2). W is the rate of mechanical work (W/m^2). *C* is the sensible heat gain or loss by convention (W/in^2). R is the sensible heat gain or loss by emitted radiation (W/m°). *Esw* is the total evaporative latent heat loss from the skin by sweat (W/m'). Cres is the convective heat gain or loss by respiration (W/m°). *Eres* is the evaporative heat loss by respiration (W/in'). *S* (W/m°) is the total storage heat flow in the body. All the terms are positive (body heating) when heat that is produced in the body and gained from the environment and negative (body cooling) when heat is lost to the environment.

In the heat balance equation, the storage flow of heat in the body, *S,* means body heating when positive and cooling when negative. When *S* is equal to 0 the amount of heat produced in the body and gained from the environment is the same as that lost to the environment, and the body temperature is in a steady state

Heat Budget on Human Body

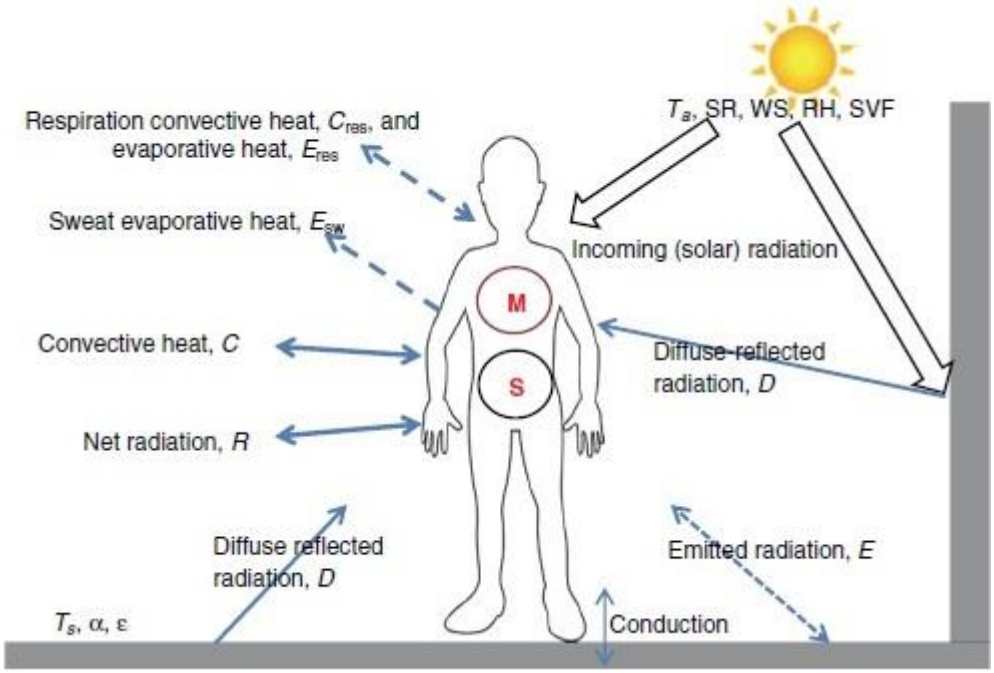

Figure 4.1. Illustration of heat budget on human body(66). (*Ts*, α and ε are temperature, albedo and emissivity of pavement or other vertical surfaces, respectively. *Ta*, *SR*, *WS*, *RH* and *SVF* are air. temperature, total solar radiation, wind speed, relative humidity and sky view factor, respectively.)

For the two-node model, the energy balance at the core and shin nodes may be written as follows (Equation 4.5 to 4.9):

$$S = S_{cr} + S_{sk} \tag{4.5}$$

$$S_{cr} = M + W + (C_{res} + E_{res}) - H_{c\text{-}s} \tag{4.6}$$

$$S_{sk} = H_{c\text{-}s} + (C + R + E_{sk}) \tag{4.7}$$

$$S_{cr} = \frac{m_{cr} c}{A_{hb}} \frac{dT_{cr}}{dt} \tag{4.8}$$

$$S_{sk} = \frac{m_{sk} c}{A_{hb}} \frac{dT_{sk}}{dt} \tag{4.9}$$

- where, *Scr* is the net heat flow to (positive, heating) or from (negative, cooling) the core in (W/m^2).
- *Ssk* is the net heat flow to (positive, heating) or from (negative, cooling) the skin in (W/m^2).
- *Mcr* and *msk* are the masses of body core and the skin, respectively in (kg). *c* is the body heat capacity in (J/kg °C).
- *Ahb* is the body surface area in (m2).
- *Tcr* and *Tsk* are the transient temperatures of the body core and the skin, respectively in (°C).
- *t* is the exposure time for assessment of human body in the thermal environment in (sec).

4.2.5 The mass and body surface area

The mass at the core and skin nodes are calculated using the fraction of the total mass, also called the effective shell thickness (n), following Gagge et al.(61,62):

$$m_{co}=(1-\alpha)Wt \quad 4.10$$

$$m_{sk}=\alpha Wt \quad 4.11$$

where *Wt* is the total body weight (kg).Mcr and Msk are mentioned in eq (4.8) and (4.9)

The body surface area is calculated from (72):

$$A_{hb}=0.203Ht^{0.725}\ Wt^{0.425} \quad 4.12$$

where Ht is the body height (m).

4.2.6 Thermal signals of human body

The thermoregulation processes are controlled through feedback thermal signals by deviations in the skin, core, and body temperatures.

The thermal signals for the skin *(TS,, ,* in °C), core *(TS,,.* in °C) and body *(FSt* , in °C) are calculated following Gagge et al.:

$$TS_{sk} = T_{sk} - 34.1 \quad 4.13$$

$$TS_{cr} = T_{cr} - 36.6 \quad 4.14$$

$$TS_{hb} = \alpha TS_{sk} + (1-\alpha)TS_{cr} \quad 4.15$$

The numeric values (34.1 and 36.6) in the above equations are the set-points for the skin and core nodes in the two-node model. The thermal signals from the skin and core are warm (positive) or cold (negative) signals to control vasodilation, vasoconstriction, blood flow and shivering, while the body thermal signal is used only when indicates warmth to regulate sweating along with the skin thermal signal for warmth.

4.2.7 ***Metabolic rate***

By the oxidation of the constituents of food (carbohydrates, fat, or proteins), energy is transformed into heat in the body. The metabolic heat production rate (*M*) is primarily dependent on the physical activity. Some examples for metabolic rates are listed in **Table 4.1**(73).

Table 4.1. Metabolic rates at different activities

Activity	Metabolic rate (met)	Metabolic rate (W/m^2)
Reclining	0.8	46
Seated, relaxed	1.0	58
Standing, light activity	1.6	93
Standing, medium activity	2.0	116
Walking on level ground, 2 km/h	1.9	110
Walking on level ground, 3 km/h	2.4	140
Walking on level ground, 5 km/h	3.4	200

1 metabolic unit = 1 met = 58 W/m^2.

With the system of the equations above, all relevant heat fluxes and thermo-physiological body limits can be calculated for any given climatic conditions considering all relevant meteorological limits. Also, comfort indices, such as SET and PET, can be calculated from these models for steady state or dynamic state.

The ASHRAE's SET index is defined as the equivalent air temperature of an isothermal environment at 50% RH in which a subject, while wearing standardized clothing for the activity concerned, would have the same heat stress (skin temperature *Tsk*) and thermoregulatory strain (skin wittedness, *w*) as in the actual environment being evaluated. The isothermal environment refers to the environment at sea level, in which the air temperature is equal to the mean radiant temperature and the air velocity are zero.

The PET is developed by a German research group headed by Peter Hoppe and is recommended as a thermal index by the German Association of Engineer's VDI guidelines (German guidelines for urban and regional planners). PET is defined as the equivalent air temperature at which, in a typical indoor setting (*Tmrt=Ta*; *VP*=12 hPa; *v*=0.1 m/s,), the heat balance of the human body is maintained with core and skin temperatures equal to those under the actual complex conditions being assessed.

Both SET and PET have a thermo-physiological background and therefore they give the real effect of the sensation of climate on human beings. Moreover, they both have the unit degree. Celsius (°C) and can therefore be more easily related to common experience and interpreted by planners for design purposes. So, both SET and PET can be used to evaluate the outdoor thermal environment. For this study, the PET is selected as a main thermal index to evaluate its effect on human thermal comfort. Analysis are done using two *different* software's through EnviMet And RayMan.(Chapter 5)

4.3 Example calculation of PET:

To demonstrate the heat balance model of a human body, through a study published in a research paper by Dr.Hui Li (66) can be discussed below:

The heat flux, body temperatures and PET were calculated for a typical hot outdoor condition and illustrated in **Figure 4.2**. In this case, an adult of 1.80 m height, 75 kg weight and with light wearing of 0.5 clo (1 clo=0.155 m2K/W), is walking at the speed of 2 km/h on a street paved with black asphalt and without shading. The weather conditions are *Ta*=38°C, *RH*=50% and *vw*=0.5 m/s. The Mean Radiant Temperature (*Tmrt*) of the surrounding is equal to 55 °C, which is very hot. The clothing temperature *Tcl* is up to 41.85 °C; the mean skin temperature *Tsk* is 37.94 °C, and the core temperature *Tcr* is 38.44 °C. The sweating rate *Rsw* is estimated as 0.14 g/m2s. The Physiological Equivalent Temperature (PET) the adult feels are 42.0 °C for this assumed context, which is very hot.

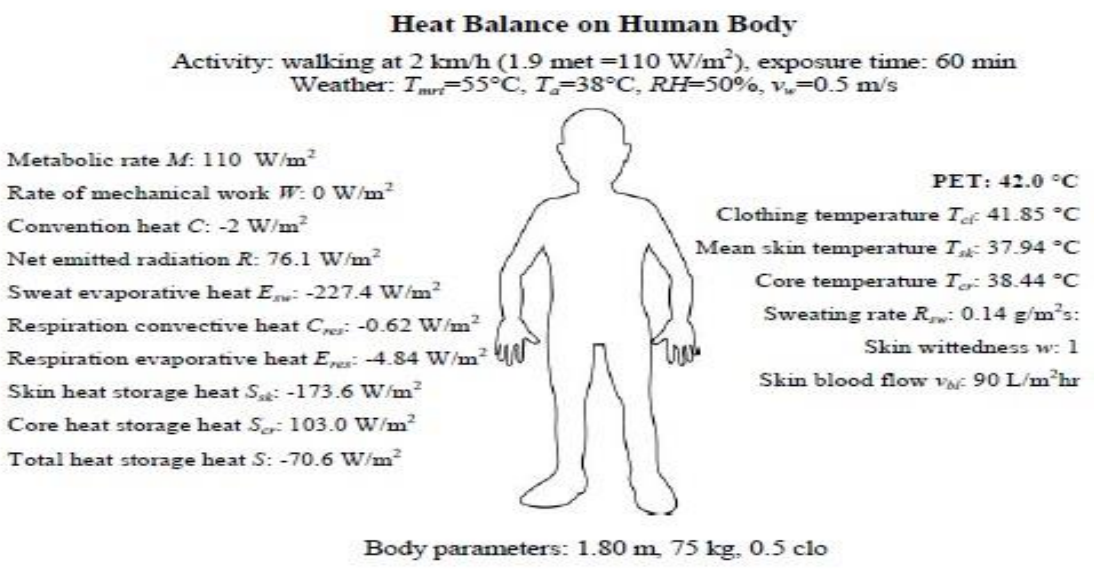

Figure 4.2. Illustration of energy balance model on human body *(66)*

Thermal sensation or subjective thermal perceptions are related to PETs. Previous studies (e.g. [38-40]) indicated that occupant thermal sensations and preferences vary for different regions due to the differences in behavioral adjustment, physiological acclimatization, and psychological habituation or expectations. This may lead to different thermal comfort ranges.

Table 4.2 lists the thermal sensation classification for different regions. The PET range for Taiwan and Western/middle European countries are from the survey studies conducted in these regions (74,75). The comparison of the thermal sensation classifications for these two regions demonstrates that the thermal comfort range in Western/middle European countries (18-23 °C PET) is lower than that of Taiwan (26-30 °C PET). People living in Western/middle European. countries cannot tolerate temperatures as high as those tolerated by people living in Taiwan with a tropical climate. The climate in Davis, California is not as hot as that in Taiwan but is hotter than that of in Western/middle European countries. so, the thermal sensation classification is. estimated for Davis, California based on those for Taiwan and Western/middle European Countries, as listed in **Table 4.2**. More accurate local thermal sensation classification for Davis, California could be obtained from outdoor field study and survey (e.g(74,75)to set up the correlation between thermal sensation and PET for local occupant.

Thermal sensation	PMV	PET range for Taiwan[a] (°C PET)	PET range for Western/Middle European[b] (°C PET)	PET range for Davis, CA (°C PET)
Very hot	>3.5	>42	>41	>40
Hot	2.5 - 3.5	38 - 42	35 - 41	35 - 40
Warm	1.5 - 2.5	34 - 38	29 - 35	30 - 35
Slightly warm	0.5 - 1.5	30 - 34	23 - 29	26 - 30
Neutral	-0.5 - 0.5	26 - 30	18 - 23	19 - 26
Slightly cool	-1.5 - -0.5	22 - 26	13 - 18	16 - 19
Cool	-2.5 - -1.5	18 - 22	8 - 13	12 - 16
Cold	-3.5 - -2.5	14 - 18	4 - 8	6 - 12
Very cold	<-3.5	<14	<4	<6

a* *Lin and Matzarakis*, b* *Matzarkis and Mayer, Davis (Hui Li,2012)*

Table 4.2: **Thermal sensation classifications for different regions**

4.4: General Pavement limits:

Heat Capacity:

Heat Capacity is the energy needed to raise a unit mass of a substance by one unit of temperature, typically expressed in units of J/kg•K. The heat capacity of dense-graded asphalt and concrete are very similar, being about 900 J/kg•K (71) which was also considered for the simulation purpose.

Thermal Conductivity:

Thermal conductivity is a measure of the ability of a material to conduct or transmit heat. It is the ratio of heat flux (power per unit area) to temperature gradient, and is expressed in units of W/m•K.

A material with a high thermal conductivity will transfer heat at a higher rate than a material having a low thermal conductivity. The thermal conductivity of pavement materials were considered as 2.0 W/m•K for asphalt and concrete (71).The value was also be considered for the simulation.

For the analysis, the value of heat capacity and thermal conductivity were kept constant for both asphalt and concrete conditions.

General Pavement thickness Design:

After selection of the type of concrete pavement type of subbase if needed, and type of shoulder (with or without concrete shoulder, curb and gutter or integral curb), thickness design is determined based on four design factors:1.Flexural strength of the concrete (modulus of rupture, MR)2.Strength of the subgrade, or subgrade and subbase combination (k)3.The weights, frequencies, and types of truck axle loads that the pavement will carry 4.Design period, which in this and other pavement design procedures is usually taken at 20 years, but may be more or less.

For the study, a heavy-duty parking lot was considered and the value of 4 inch in the thickness option(y grid)in simulation was considered for the simulation in Envimet and Rayman.

Large flat paved area (e.g. parking lots.) was used to evaluate and compare the effects of two different pavement surfaces (asphalt and concrete) through microclimate analysis in Envimet and Rayman for summer climate (Sacramento region). Standard parameters (mentioned in table 4.3 to 4.6) for asphalt and concrete were used and Weather data for summer (June and July) climate were considered for the simulation scenarios.

4.5 Models followed by Envimet and Rayman Software

4.4.1 ENVI-met Details:

ENVI-met v5, one of the most widely used Computational Fluid Dynamics (CFD) software for urban microclimate simulations on a global scale, has been validated in many countries.In addition to considering variables such as solar radiation, wind, soil, and vegetation, it uses the Biomet tool to calculate comfort indexes and allows the definition of materials by thermal characteristics, such as albedo and emissivity, which makes it appropriate for the analysis of the impact of albedo on the thermodynamic performance of the selected area and on users' comfort in this study. ENVI-met uses the Finite Difference numerical method to solve the multitude of partial differential equations (PDE) and other aspects in the model. Its accuracy has been tested in terms of the thermal performance of the outdoor environment, particularly on a large scale. Envimet simulates the surface-plant air interactions in an urban environment(56). It is validate and compared to onsite measurements(76)..Envimet calculation of MRT is defined by the following equation (56).

The surrounding environment consists of the building surfaces,the atmosphere and the ground surface.All radiation fluses,i.e. direct irradiance It(z),diffuse and diffusely reflected solar radiation Dt(Z) as well as the total long-wave radiation fluxes Et(z) from the atmosphere, ground and walls, are taken into account(73).At street level, Et(z) is assumed to be originated 50% from the upper hemisphere (sky and buildings) and 50% from the ground. This approximation is valid only at street because of the influence of longwave radiation of the ground decrease with the increased height. The temperature of each building surface viewed from the face of a target point is calculated as a weighted temperature, where the weight is defined by how much surrounding surfaces are viewed by the face of a given point.

$$T_{mrt} = \left[\frac{1}{\sigma} \cdot \left(E_t(z) \cdot \frac{a_k}{\epsilon_p} \cdot \left(D_t(z) + I_t(z)\right)\right)\right]^{0.25} \text{[K]} \quad 4.16$$

In equation 4.16, σ is the Stefan- Boltzmann constant, I= direct irradiance = Non-scattered solar radiation D=Long Wave solar radiation E=radiation from the atmosphere, ak=body absorption coefficient, εp (-) is the emissivity of human body.

The Stefan-Boltzmann constant, ($5.670374419 \times 10^{-8}$ watt per square meter per kelvin to the fourth ($W / (m^2 \times K^4)$ symbolized by the lowercase Greek letter sigma (σ), is a physical constant expressing the relationship between the heat radiation emitted by a black body and its absolute temperature. σ represents the constant of proportionality between these two variables.

4.6 Envimet simulation

Envi-met Modelling software input and Methodology:

The ENVI-met is a three-dimensional micro-scale thermal model that analyzes the interactions of various elements within an urban environment. The software inputs various limits such as building structure, vegetation, ground surfaces, climatic conditions, and soil, and simulates the changes from proposed building forms, shading, orientation, and other modifications. The ENVI-met model takes into account the fluid dynamics of air flow and turbulence, as well as thermodynamic processes occurring at various surfaces such as the ground, walls, roofs, and plants. The software considers all types of solar radiation and calculates the mean radiant temperature, including the effect of plant shading, absorption, and re-radiation. The cell area for simulation can vary from 0.5 meters to 10 meters and the simulation is processed using both the input and configuration files. The output data is then imported into the LEONARDO 3.0 visualization program where it can be visualized in plan, section, or 3-D axonometric views. The main layers used for visualization include data layer for continuous data display, special layer for singular data display, and vector layer for wind display.

Methodology:

- Microclimate simulation was conducted in Envi-met for the purpose of using the information into Rayman for albedo optimization.(Figure 4.3 to Figure 4.6)

Figure: 4.3 Location for Asphalt based Analysis (A hypothetical location similar to Sacramento bridge area parking lot was considered for the simulation area in EnviMet)

Figure 4.4 Location Concrete-based Analysis(A location similar to Davis/Sacramento concrete area parking lot was considered for the simulation area)

Figure:4.5 Building 3-D model in Envimet

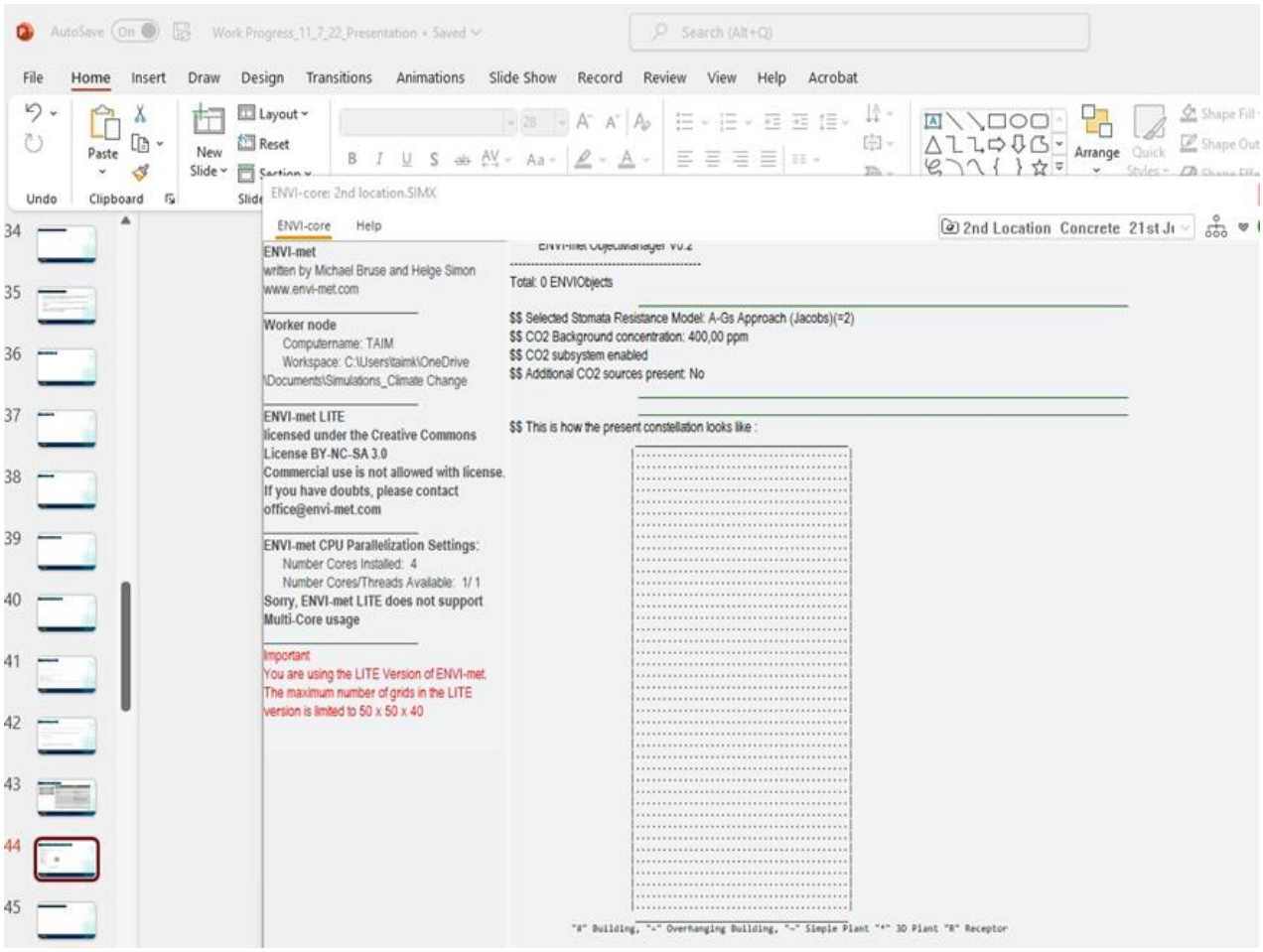

Figure 4.6: Simulation in Envimet

- The hypothetical sites in Sacramento were simulated using ENVI-met models (v5) based on the actual environment.
- ENVI-met modelling software was used to establish a numerical model of pavement sections, incorporating temperature, wind speed, humidity and pavement properties.(figure 4.3 to figure 4.6).

  For simplification, Two pavement sections of asphalt(table 4.7 and 4.9) and concrete (table 4.8 and 4.10) were selected for the analysis in EnviMet and in RayMan and specific inputs(table 4.3 to 4.6) were provided for the simulation for the date June 21st to June 24th and from July 15th to July 18th 2022.So in total four different scenarios will be part of the simulation and analysis process as follows:

A. Analysis of Asphalt based flat (parking area) for June 21st to June 24th 2022 Simulation input Table 4.7

B. Analysis of Concrete based flat (parking area) for June 21st to June 24th 2022 Simulation input Table 4.8

C. Analysis of Asphalt based flat (parking area) for July 15th to July 18th 2022 Simulation input table 4.9

D. Analysis of Concrete based flat (parking area) for July 15th to July 18th 2022 Simulation input table 4.10

- Table 4.3 to 4.10 mentioned in this chapter shows the input details in EnviMet,3D model building, simulation.
- The pavement simulation area was defined as a 40*40*30 m square and implemented with an open boundary condition and a terrain height of 3 m. No building height was considered as a flat parking lot was selected, without vegetation.
- After simulation was run, it was processed using both input and configuration files and the output data was imported and visualized in LEONARDO 5 (Shown in appendix tables A-1 to A 10,B1 to B 10,C1 to C10 and D1 to D 10).
- After conducting the simulation, results were collected for further analysis in RayMan where optimization of albedo was conducted (mentioned in chapter 5).

Simulation inputs for different scenarios for Envimet:

Table 4.3 Asphalt Pavement Input details: For Date:21st June to 24th June and 15th July to 18th July

Pavement Property	**Value**
Roughness length	**.01**
Albedo	**.2 (Envimet uses the default albedo value and does not allow to change the albedo value)**
Emissivity	**.9**

Table 4.4:Concrete Pavement Inputs:For Date:21st June to 24th June and 15th July to 18th July

Pavement Property	**Value**
Roughness length	**.01**
Albedo	**.5**
Emissivity	**.9**

Altitude: .2 to 10 m (For both asphalt and concrete)

Heat Capacity: 900 J/kg•K(For both asphalt and concrete)

Conductivity: 2.0 W/m•K (For both asphalt and concrete)

Personal Data	Values
Height	1.75m for adult, .9m for child
Weight	75 kg for adult,15kg for child
Age	35 for adult (3 to 9 for child)
Sex	Male and Female (adult and child)

Table: 4.5 Personal Data Input

Clothing and activity(for adult and child)	Values
Clothing	.9
Activity	80 W
Positioning	Standing

Table 4.6: Clothing and activity input

Input details	Asphalt
Date of Analysis	**06-21-22 to 06-24-22**
Simulation Duration	**72 hours**
Start time	**9:00 am,06-21-22**
End time	**8:59 am,06-24-22**
Weather Parameters used	**Min temp-19degree(66F,5:53am 22nd June),Max-39 degree(103F,3:53pm21st June)** **Min Rel Humidity:7%(5:53pm),Max-45%(11:53pm)**
Rest of the settings	**Default (40*40*30)**

Table 4.7 Input for Scenario A in Envimet : asphalt condition (June 21st to June 24th,2022)

Condition	Concrete
Date of Analysis	06-21-22 to 06-24-22
Simulation Duration	72 hours
Start time	9:00 am,06-21-22
End time	8:59 am,06-24-22
Weather Parameters used	Min temp-19degree(66F,5:53am 22nd June),Max-39 degree(103F,3:53pm21st June) Min Rel Humidity:7%(5:53pm),Max-45%(11:53pm)
Rest of the settings	Default (40*40*30)

Table 4.8 Input for Scenario B in Envimet: concrete condition (June 21st to June 24th,2022)

Condition	Asphalt
Date of Analysis	07-15-22 to 07-18-22
Simulation Duration	72 hours
Start time	9:00 am,07-15-22
End time	8:59 am,07-18-22
Weather Parameters used	Min temp-19degree(66F,5:53am 22nd June),Max-39 degree(103F,3:53pm21st June) Min Rel Humidity:7%(5:53pm),Max-45%(11:53pm)
Rest of the settings	Default (40*40*30)

Table 4.9: Input for Scenario C in Envimet: asphalt condition(July 15th to July 18th,2022)

Condition	Concrete
Date of Analysis	07-15-22 to 07-18-22
Simulation Duration	72 hours
Start time	9:00 am,07-15-22
End time	8:59 am,07-18-22
Weather Parameters used	Min temp-19degree(66F,5:53am 22nd June),Max-39 degree(103F,3:53pm21st June) Min Rel Humidity:7%(5:53pm),Max-45%(11:53pm)
Rest of the settings	Default (40*40*30)

Table 4.10 Input for Scenario D in Envimet: concrete condition (July 15th to July 18th, 2022)

Simulation Output: Output of the Envimet simulation are shown in appendix A-1 to A-10,B-1 To B-10,C-1 to C-10 and D-1 to D-10. The output of the simulations were later used in Rayman Modelling for optimizing albedo.

4.7 Sample Simulation:

Elevation/Altitude: .2 to 10m range were selected (default value of envimet) to incorporate standard simulation timeframe and accuracy of the models in Envimet. The default elevation range of 0.2 to 10 meters used in these models is based on the fact that most outdoor activities occur within this height range and the range enables the model to capture the effects of vertical mixing and turbulent transport of heat and moisture (56).

Albedo Value	PPD(Predicted percentage of dissatisfaction	Satisfaction Percentage
0.2(Asphalt)	85	15
0.5(Concrete)	75	25

Table 4.11 Sample Envimet Simulation

4.8 Sample Simulation Result

From sample simulation of Envimet (Table 4.11), it can be understood that with different values of albedo used for the simulation, the predicted percentage of dissatisfaction was achieved and thus the satisfaction percentage was found. For Example,For Envimet Simulation,when the asphalt albedo was .2,predicted percentage of dissatisfaction was found to be 85% meaning the satisfaction percentage as 15%.

And for concrete simulation, when the concrete albedo was .5,the predicted percentage of dissatisfaction was found to be 75 and the satisfactions percentage was 25%.The results indicate that with variation of albedo, satisfaction level also changes. Thus indicating the relationship of albedo with human thermal comfort.

Thus the Enivmet sample results suggest that albedo of concrete could result in higher thermal comfort for human beings rather than Asphalt. Overall, the findings suggest that the variation albedo of surfaces in urban environments can significantly impact the levels of human thermal comfort.

4.9 **Use of Envimet Simulation results for optimization in Rayman**

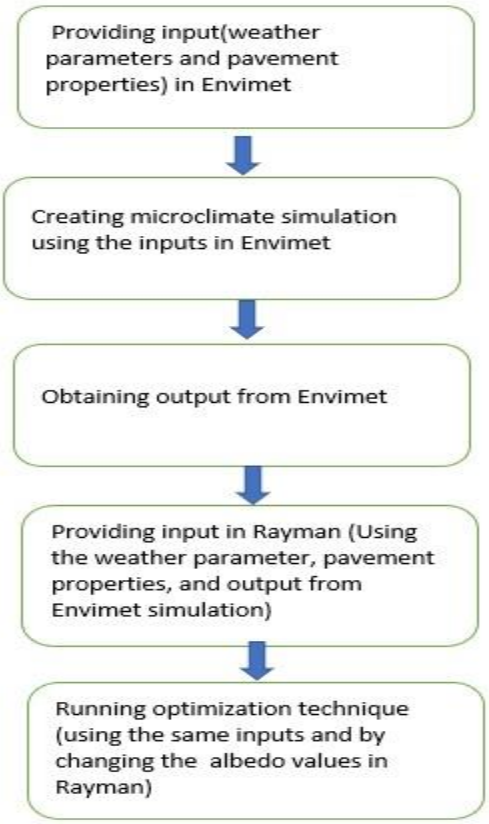

Figure 4.7:A flowchart showing interaction between Enivmet and Rayman

Some of the the Envimet simulation outputs(PET,MRT) were used for conducting optimization process in Rayman to be showed in chapter 5. Figure 4.7 shows the interaction between Envimet and Rayman.

Chapter 5: Analysis and Findings: Optimization of Albedo for Human Thermal Comfort using Rayman Modelling software:

5.1 The RayMan model:

The goal of the chapter is to discuss the process of albedo optimization for human thermal comfort. Since Envimet does not allow to change albedo, another microclimate simulation called Rayman would be used for the optimization technique. Developed for the calculation of the mean radiation temperature and thermal indices in simple and complex environments, is only based on data of air temperature, air humidity and wind speed (68). RayMan can be used for the assessment of urban bioclimate and thermal indices such as Predicted Mean Vote (PMV), Physiologically Equivalent Temperature (PET) and Standard Effective Temperature (SET*). The model is developed based on the German VDI-Guidelines 3789, Part II: Environmental Meteorology, Interactions between Atmosphere and Surfaces; Calculation of the short- and long wave radiation and VDI-3787: Environmental Meteorology, Methods for the human-bio meteorological evaluation of climate and air quality for the urban and regional planning at regional level. Part I: Climate. Detailed calculation for thermal comfort and human energy fluxes based on the **M**unich **E**nergy Balance **M**odel for **I**ndividuals (MEMI)(68). Some of the output values of Envimet simulation such as PET,MRT(Mean radiant temperature) would be used for the optimization process in Rayman .Since, PET and MRT values were not found from any other source, Envimet simulation output values were used for the purpose to run the optimization in Rayman.

5.1.1 Input details for Rayman:

Table 5.1:Concrete Pavement Inputs for Date:21st June to 24th June and 15th July to 18th July

Pavement Property	Value
Roughness length	.01
Albedo	.05,.1,.15,.2,.25,.3,.35,.4,.45,.5
Emissivity	.9

Altitude: .2 to 10 m

Heat Capacity: 900 J/kg•K

Conductivity: 2.0 W/m•K

Other Inputs:

Weather Inputs	**Table Number(All tables are in Appendix)**
Air Temperature	Table AA1, AA2
Humidity	Table AA3, AA4
Surface Temperature	AA7 to AA10
Wind Velocity	AA5 and AA 6
Mean Radiant Temperature	A1,B1,C1 and D1

Table 5.2: Weather Input

Personal Data	**Values**
Height	1.75m for adult, .9m for child
Weight	75 kg for adult (15kg for child)
Age	35 for adult (3 to 9 for child)
Sex	Male and Female (adult and child)

Table: 5.3 **Personal Data Input**

Clothing and activity (both adult and child)	
Clothing	.9
Activity	80 W
Positioning	Standing

Table 5.4: **Clothing and activity input**

5.2 Optimization of Albedo:

After getting the PET and MRT values from Envimet simulation, RayMan software was used for the optimization Technique ,keeping heat capacity and conductivity constant, only albedo was optimized for human thermal comfort.

Methodology: Optimizing Albedo for Human Thermal Comfort using RayMan Model

1. Albedo inputs were provided into the RayMan model with values ranging from 0.05 to 0.5 with an interval of 0.05.(Figure 5.1 to Figure 5.3)
2. Individual Pavement properties were provided for concrete and Mean Radiant Temperatures, Wind Speed, Relative Humidity and Air Temperature were kept constant during the simulation, only surface temperatures of Asphalt and Concrete were changed.(Table 5.1 to Table 5.4)

   3.Heat Capacity: Heat Capacity is the energy needed to raise a unit mass of a substance by one unit of temperature, typically expressed in units of J/kg•K. The heat capacity of asphalt and concrete are very similar, being about 900 J/kg•K which was the default value for the simulation purpose. (35)

4. Thermal conductivity is a measure of the ability of a material to conduct or transmit heat. It is the ratio of heat flux (power per unit area) to temperature gradient, and is expressed in units of W/m•K. A material with a high thermal conductivity will transfer heat at a higher rate than a material having a low thermal conductivity. The default thermal conductivity of asphalt and concrete pavement materials was 2.0 W/m•K and was kept same for both for the simulation.

5.The simulation was constructed for 3 day duration for each month of June and July (21st to June 24th and July 15 to July 18th).

6.The optimization process was performed by observing the peak Predicted Percentage of Dissatisfaction (PPD) changes for different inherent albedo values.

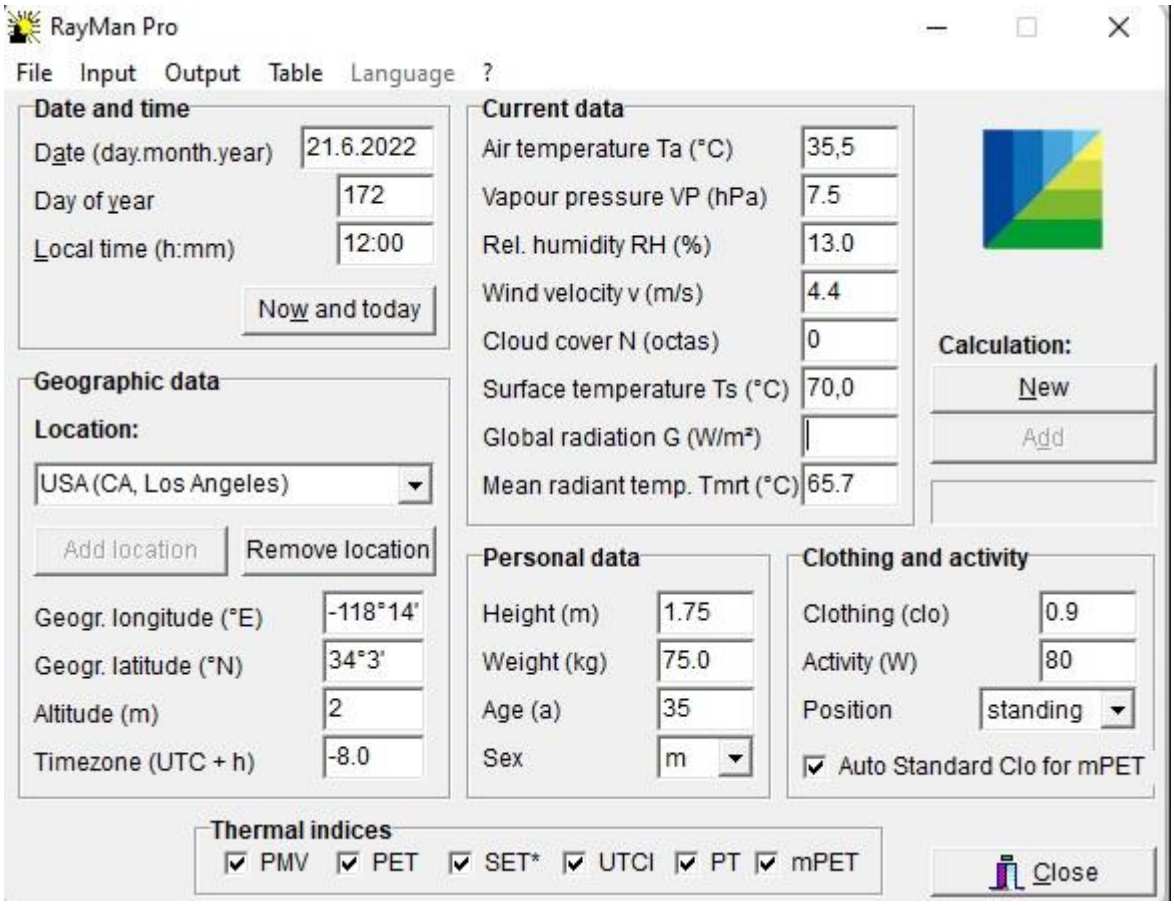

Figure:5.1 Simulation Input

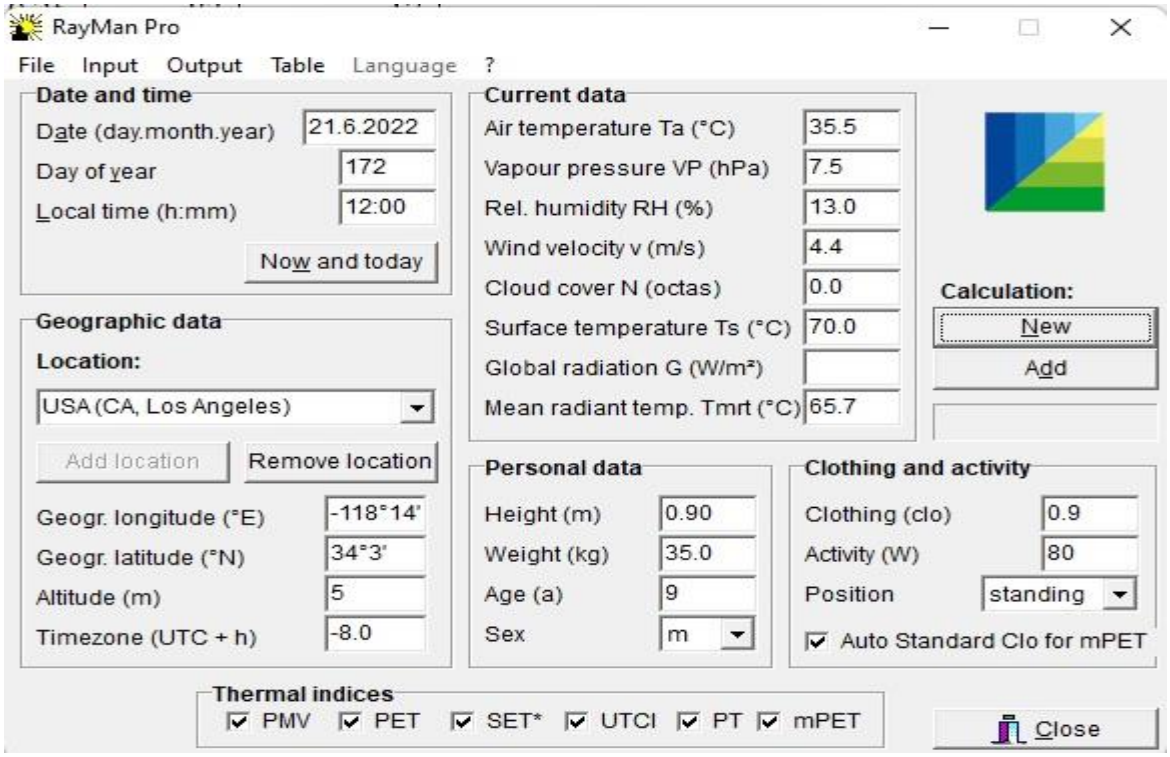

Figure: 5.2 Simulation Input

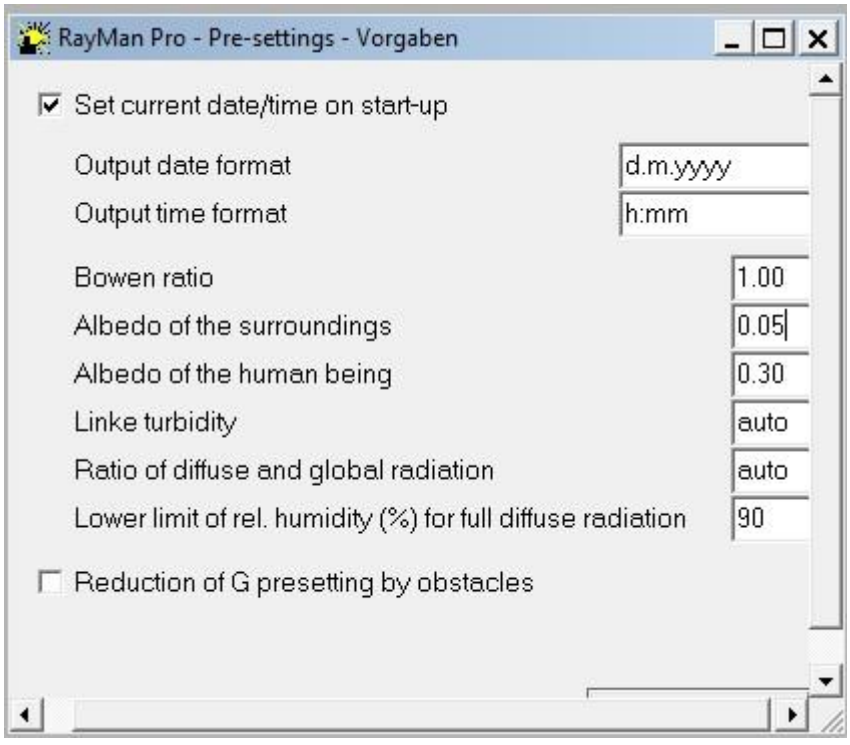

Figure 5.3: Optimization of albedo

5.3 Initial Simulation output:

Scenario A:Concrete: Condition: June 21st to June 24th (For both adult and children)

The following table shows the albedo values from .05 to .5 with an increment of .05.

Albedo Value	PPD(Predicted Percentage of Dissatisfaction)	Satisfaction Percentage
0.05	85	15
0.1	76	24
0.15	68	32
0.2	81	19
0.25	84	16
0.3	85	15
0.35	89	11
0.4	90	10
0.45	88	12
0.5	90	10

Table 5.5: **PPD Vs Albedo,** (Concrete: Condition: June 21st to June 24th)

Scenario B:Concrete Condition: July 15th to July 18th (For both adult and children)**.**The following table shows the albedo values from .05 to .5 with an increment of .05.

Albedo Value	PPD(Predicted Percentage of Dissatisfaction)	Satisfaction Percentage
0.05	89	11
0.1	80	20
0.15	68	32
0.2	81	19
0.25	85	15
0.3	88	12
0.35	91	9
0.4	93	7
0.45	88	12
0.5	86	14

From sunrise to sunset (from 6am to 8pm)

Table 5.6: **PPD Vs Albedo, (**Concrete Condition: July 15th to July 18th)

5.4: Findings from the optimization :

The Rayman model optimization results provide important insights into the optimal albedo value for achieving maximum thermal comfort. The graphs presented in figures 5.4 to 5.5 show the relationship between the albedo value and the percentage of dissatisfaction value. The x-axis represents the albedo value, and the y-axis represents the percentage of dissatisfaction value.

Upon analyzing the graphs, it becomes apparent that the optimal albedo value is 0.15, where the lowest amount of dissatisfaction was observed. This result indicates that at an albedo value of 0.15, people will experience the least amount of thermal discomfort, resulting in the highest level of thermal comfort. Furthermore, the results show that at this optimal albedo value, a maximum thermal comfort of 30% was achieved for the 72-hour duration.

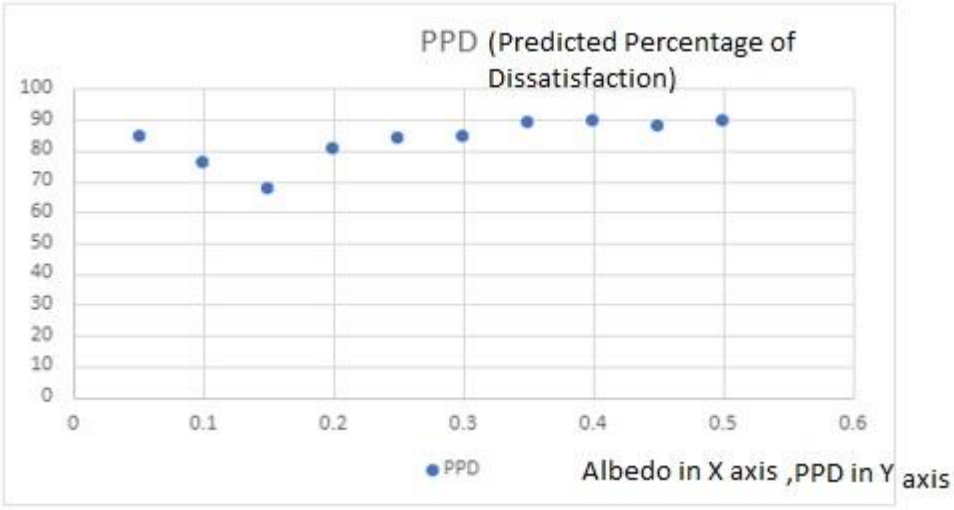

Figure:5.4 :Individual PPD percentage for concrete condition for June 21st to June 24th:

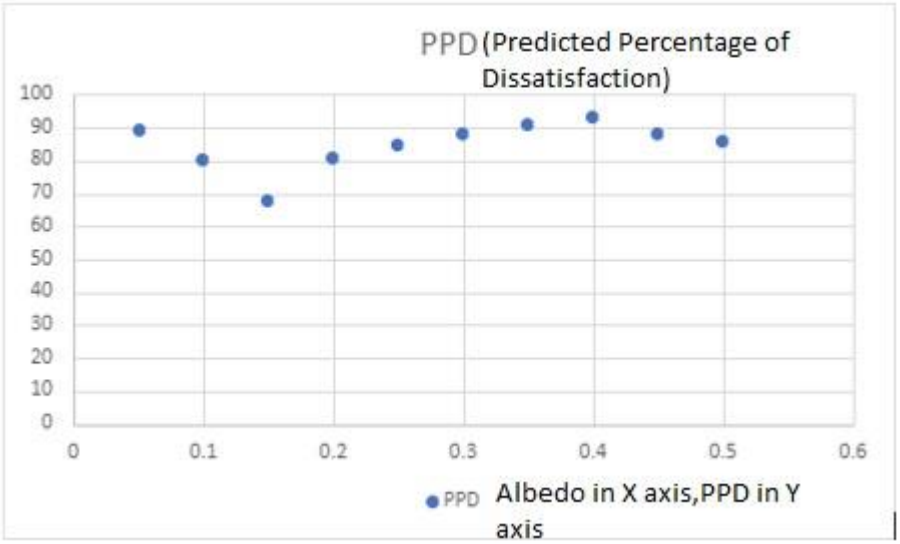

Figure: 5.5 Individual PPD percentage for concrete condition for July 15th to July 18th

5.5: Limitation of the optimization technique:

 Inability to determine the exact time when the satisfaction percentage was achieved - The simulation was only able to provide the greatest value of ppd that can occur within a 72-hour period, which means that the exact time when the satisfaction percentage was achieved is not known.

 Limited time period - The optimum albedo value found in the simulation was only based on the findings from June and July of 2022. It is unclear whether the albedo values for other months would be the same, which limits the generalizability of the findings.

 Limited scope - The study only focused on the impact of pavement albedo on pedestrian comfort, and other factors that can affect pavement performance, such as durability, safety, and cost, were not considered.

5.6 Recommendation regarding the optimum albedo: There are some of the limitations of the study, such as the limited time period and correlation of data, make it difficult to generalize the findings to other months of the year when weather parameters may be different. Future studies that take into account a wider range of weather conditions and pavement materials may help to provide a more comprehensive understanding of the optimal pavement albedo values for different contexts.

5.7 Discussion based on the optimization processes in Rayman: While the results of this study suggest that optimizing pavement albedo can have a significant impact on pedestrian thermal comfort, it is important to note that other factors may also play a role. Mean radiant temperature, surface temperature, physiological equivalent temperature, and humidity are all important variables that can affect human thermal comfort. Mean radiant temperature, for example, measures the average temperature of all surfaces surrounding a person, while surface temperature is the temperature of the ground or pavement. Physiological equivalent temperature is a measure of how hot or cold a person feels based on the combined effects of air temperature, humidity, radiation, and air velocity, while humidity can affect how much moisture is evaporated from the skin, which can impact thermal comfort. Therefore, in order to fully understand the impact of pavement albedo on human thermal comfort, it may be necessary to take these other factors into consideration in future studies.

Further research for different time with additional data and continuous development of Envimet and Rayman software is required to fully understand the relationship between albedo and human thermal comfort.With the development of the softwares will lead towards conducting the simulation in faster time and receiving quicker results. Thus, it will be highly beneficial for future studies.

5.8: Correlation analysis:

Correlation analysis is an important tool for understanding the relationship between variables, including the relationship between human thermal comfort and variables such as mean radiant temperature, physiological equivalent temperature, and albedo.

Mean radiant temperature, physiological equivalent temperature, and albedo all have a significant impact on human thermal comfort, as they are all related to the amount of heat that a person perceives in their environment.

Researchers can make predictions and create interventions aimed at enhancing comfort by using correlation analysis to evaluate the degree and direction of the association between these variables to predict thermal comfort.

For example, if a high correlation is found between mean radiant temperature and human thermal comfort, this could show that controlling mean radiant temperature is an effective way to influence comfort levels. Conversely, if a low correlation is found, it may suggest that other factors are more important in determining thermal comfort.

In summary, conducting a correlation analysis between human thermal comfort and variables such as mean radiant temperature, physiological equivalent temperature, and albedo is important for understanding the factors that impact thermal comfort and for developing strategies to improve it.

5.9 Wind Speed and Correlation:

Wind speed is an important factor to consider in evaluating human thermal comfort because it can have a significant impact on how a person perceives the temperature of their environment. Wind can increase heat loss from the body and can increase the evaporation of sweat, leading to a feeling of coolness and discomfort. On the other hand, too much wind can cause discomfort due to turbulence and air movement.

A correlation analysis between wind speed and human thermal comfort can help to understand the relationship between these two factors and the impact of wind speed on comfort levels. If a strong correlation is found, it can show that wind speed is a key factor in determining thermal comfort and should be carefully considered in the design of environments where people spend time. On the other hand, if a weak correlation is found, it may suggest that wind speed is not a significant factor in thermal comfort and that other factors should be given greater consideration.

In conclusion, considering the impact of wind speed on human thermal comfort is important as it can significantly influence how comfortable a person feels in their environment. Correlation analysis can help to understand the relationship between wind speed and thermal comfort and inform design decisions to improve comfort levels. It can be understood that wind speed is an important parameter for human thermal comfort, and its impact on thermal sensation has been extensively studied. Research (67) shows that as wind speed increases, people can tolerate higher air temperatures due to the evaporative cooling effect on the skin. This knowledge has important implications for designing and managing built environments, especially in hot climates.

Along with optimization of albedo, correlation analysis was conducted to find the influence of mrt, pet and wind speed on human thermal comfort.The Pearson correlation method was used to perform a correlation analysis between human thermal comfort and the factors of Physiological Equivalent Temperature (PET), Mean Radiant Temperature (MRT), and Wind Speed. This method allows for the assessment of the linear relationship between two variables. By using the Pearson correlation method, the researchers aimed to gain a deeper understanding of how these factors contribute to human thermal comfort and to determine which variables have the strongest relationship with it.

The results of this analysis can offer valuable information for improving the outdoor environment and enhancing the thermal comfort of occupants.

This approach using statistical analysis can help make data-driven decisions and improve the comfort of people in different environments.

Data for correlation:

Table AA5 and AA6 of wind speed for both asphalt and concrete condition and table A5,B5,C5 and D5 were used for the PET adult condition, table A6,B6,C6 and D6 were used for PET child condition. Table A1, B1, C1 and D1 were used for MRT data.Table A-5 and Table A-6 has been shown here. Analysis was conducted using these tables for finding out the correlation.

Table A-5

PET(Adult): The following table shows PET values for the time 21st June,9:00 am to 24th June 9: have been plotted. We can see the variation of values hereby in the table. The values increase in the early morning to reach peak value around 5 pm.

Time	21St June-22nd June (Temp in Degree C)	22nd June-23rd June (Temp in Degree C)	23rd June-24th June (Temp in Degree C)
9 am	13.3	13.6	13.6
10 am	18.9	18.8	18.9
11 am	23.6	23.7	23.8
12 pm	30.5	30.2	30.4
1 pm	32	33	33.2
2 pm	33	33.4	33.5
3 pm	33.5	33.5	33.6
4 pm	34.5	34.7	34.8
5 pm	34.6	34.8	35
6 pm	34.4	34.9	34.1
7 pm	32	32.4	33
8 pm	31	31.4	32,2
9 pm	21.8	21.9	22.3
10 pm	20	20.4	20.6
11 pm	19	19.5	19.7
12 pm	19	19.4	19.7
1 am	18	18.5	18.8
2 am	17.5	17.6	17.9
3 am	16	16.4	17.1
4 am	17	17.4	18.1
5 am	17.5	17.6	18.2
6 am	19	19.6	20.1
7 am	20	20.6	20.8
8 am	22	22.4	22.6

Table A-6

PET(Child)

The following table shows PET values for the time 21st June,9:00 am to 24th June 9: have been plotted. We can see the variation of values hereby in the table. The values increase in the early morning to reach peak value around 6 pm.

Time	21St June-22nd June (Temp in Degree C)	22nd June-23rd June (Temp in Degree C)	23rd June-24th June (Temp in Degree C)
9 am	13.5	13.8	14.1
10 am	19.1	18.9	19.2
11 am	23.7	23.9	24.2
12 pm	30.6	30.8	31.4
1 pm	32.1	32.5	33.7
2 pm	33.4	33.9	34
3 pm	33.9	33.8	34.1
4 pm	34.8	34.9	35.1
5 pm	34.9	35.2	36
6 pm	34.7	35.3	34.6
7 pm	32.4	33	33.4
8 pm	31.4	31.8	32,7
9 pm	21.9	22.4	22.8
10 pm	20.5	20.9	20.8
11 pm	19.4	20.1	20.4
12 pm	19.9	19.7	20.2
1 am	18.4	19.1	20.3
2 am	17.7	18.2	18.5
3 am	16.8	17.2	17.6
4 am	17.5	18.2	18.4
5 am	17.9	18.4	18.8
6 am	19.2	20.3	20.9
7 am	20.5	20.9	21.3
8 am	22.8	22.8	22.9

For Table 5.7, MRT data were used rom Appendix A1, B1, C1 and D1

Human Thermal Comfort Data were used from Appendix table A-9, B 9, C9 and D-9

Date	Correlation between MRT and Human Thermal Comfort	Relationship	Positivity/negativity
June 21st to June 24th 2022	-.46	Weak	Negative
June 21st to June 24th 2022	-.47	Weak	Negative
July 15th to July 18th 2022	-.51	weak	Negative
July 15th to July 18th 2022	-.53	Weak	Negative

Table:5.7: Correlation between MRT and Human Thermal Comfort (Adult)

For table 5.8,PET data for adult were used from appendix Table A5,,B5,C5, and D5

Human Thermal Comfort Data were used from appendix table A9,B9,C9 and D9

Date	Correlation between PET and Human Thermal Comfort	Relationship	Positivity/negativity
June 21st to June 24th 2022	-.993	Strong	Negative
June 21st to June 24th 2022	-.992	Strong	Negative
July 15th to July 18th 2022	-.997	Strong	Negative
July 15th to July 18th 2022	-.976	Strong	Negative

Table 5.8: Correlation between PET and Human Thermal Comfort (Adult)

For table 5.9, Wind speed data were used from Appendix AA5 (21st June to june24th) and AA6(15th July to 18th July).Human Thermal Comfort Data were used from Appendix A9, B9, C9 and D9

Date	Correlation between Wind Speed and Human Thermal Comfort	Relationship	Positivity/negativity
June 21st to June 24th 2022	-.723	Moderate to Strong	Negative
June 21st to June 24th 2022	-.721	Moderate to Strong	Negative
July 15th to July 18th 2022	-.75	Moderate to Strong	Negative
July 15th to July 18th 2022	-.76	Moderate to Strong	Negative

Table 5.9: Correlation between Wind Speed and Human Thermal Comfort (Adult)

Wind can affect human thermal comfort in several ways:

1. Cooling effect: Wind can help to dissipate heat from the body, leading to a cooling effect. but, if the wind is too strong, it can also cause the body to lose heat too quickly, leading to a decrease in thermal comfort.
2. Evaporation: Wind can also increase the evaporation rate of sweat on the skin, which can help to regulate body temperature and increase thermal comfort. but, if the wind is too strong, it can also dry out the skin and reduce its ability to regulate temperature, leading to a decrease in thermal comfort.
3. Air movement: Wind can also create air movement that can disrupt the layer of still air surrounding the body, which helps to insulate the body and keep thermal comfort. If the wind is too strong, it can mix warm and cool air, reducing the insulating effect and leading to a decrease in thermal comfort.

Overall, wind can have both positive and negative effects on human thermal comfort, and the net impact will depend on the wind speed, temperature, and humidity conditions. Generally, moderate wind speeds can help to improve thermal comfort, while extremely high wind speeds can have the opposite effect.

Thus, it’s important to understand the effect of wind speed on human thermal comfort.

For Table 5.10, MRT data were used rom Appendix A1, B1, C1 and D1

Human Thermal Comfort Data were used from Appendix table A-10, B 10, C10 and D-10

Date	Correlation between MRT and Human Thermal Comfort	Relationship	Positivity/negativity
June 21st to June 24th 2022	-.48	Weak	Negative
June 21st to June 24th 2022	-.49	Weak	Negative
July 15th to July 18th 2022	-.53	Weak	Negative
July 15th to July 18th 2022	-.54	Weak	Negative

Table:5.10: Correlation between MRT and Human Thermal Comfort (Child)

For Table 5.11, PET data for child were used from appendix Table A6,,B6,C6, and D6

Human Thermal Comfort Data were used from Appendix table A-10,B 10,C10 and D-10

Date	Correlation between PET and Human Thermal Comfort	Relationship	Positivity/negativity
June 21st to June 24th 2022	-.994	Strong	Negative
June 21st to June 24th 2022	-.993	Strong	Negative
July 15th to July 18th 2022	-.997	Strong	Negative
July 15th to July 18th 2022	-.978	Strong	Negative

Table 5.11: Correlation between PET and Human Thermal Comfort (Child)

For Table 5.12, Wind speed data were used from Table AA5 and AA6.

Human Thermal Comfort Data were used from Appendix table A-10, B 10, C10 and D-10

Date	Correlation between Wind Speed and Human Thermal Comfort	Relationship	Positivity/negativity
June 21st to June 24th 2022	-.73	Moderate to Strong	Negative
June 21st to June 24th 2022	-.723	Moderate to Strong	Negative
July 15th to July 18th 2022	-.76	Moderate to Strong	Negative
July 15th to July 18th 2022	-.77	Moderate to Strong	Negative

Table 5.12: Correlation between Wind Speed and Human Thermal Comfort (Child)

Correlation analysis findings

1.Three Variables were considered for the purpose MRT and PET and Wind.

2.Next, correlation analysis was done for MRT with human thermal comfort and PET with human thermal comfort also with Wind Speed with human thermal comfort.

3.MRT is poorly correlated with Human Thermal Comfort (Inverse Correlation -.46 to -.53, Highest for July).(table 5.7 and 5.10)

4.PET is strongly correlated with Human Thermal Comfort(Correlation -.97 to-.985).The lower the value of PET, The higher the human thermal comfort is.(table 5.8 and 5.11)

5.Wind speed is moderate to strongly correlated with human thermal comfort. Human Thermal Comfort increases with decreased wind speed. (Table 5.9 and 5.12)

Designers may use such correlation results with computational tools and simulation models to evaluate different design options and optimize the thermal comfort of their designs. Ultimately, the correlation between these variables and human thermal comfort can guide pavement designers in creating outdoor spaces that are not only functional but also promote the health and well-being of pedestrians.

5.10: Overall Results from environment and Rayman:

1..Based on envimet results(Appendix, table A-9,A -10,B-9,B10,C-9,C10,D-9 and D-10),it can be found that human thermal comfort of an adults are higher than human thermal comfort of children The ratio of body mass to surface area, also known as body surface area, could have affected the amount of heat transfer between the body and the surrounding environment. Children generally have a larger body surface area about their mass, compared to adults, meaning that they are more susceptible to heat transfer and may feel more discomfort in tropical environments. In addition to body surface area, other factors such as clothing, activity level, and personal tolerance for heat could also affect an individual's level of discomfort in a given environment. It is important to consider all these factors when evaluating comfort levels for different populations.

2. Based on rayman results(table 5.6 to 5.9,)Human thermal comfort of adults and children did not show any significant differences.

3..Elevation or Model height(from ground surface to above) did not play any significant effect on human thermal comfort(for the considered height of .2m to 10m).

4.The optimization technique provided the value of .15 as the optimum value for albedo.

5. The study found the optimum albedo value as .15.But the study has some limitations, such as the short time span and correlation of larger set of quantitative data, make it challenging to extrapolate the results to other months of the year when weather parameters may differ. Future studies that take into account a wider range of weather conditions and pavement materials may help to provide a more comprehensive understanding of the optimal pavement albedo values for different contexts.

6.Based on the analysis, it can be seen that human thermal comfort is also affected through PET and wind speed . Higher wind speeds result in less water evaporation and lower humidity. Low humidity can cause dry skin, irritate the nasal passages and throat, and make the eyes itchy. Thus, creating thermal discomfort. So wind speed is an important factor in human thermal comfort along with PET for human thermal comfort.

5.11 :Finally The study successfully found answers for the following questions:

(i)Can the EnviMet model give the desired result/output that can be used for albedo optimization?

The environment model gave radiation and PET values which played a significant role in optimizing Albedo in RayMan software.

(ii)Can EnviMet/RayMan allow albedo to be changed?

The models allow a peak sunlight albedo and then estimate how albedo changes with sunlight angle through rest of day. But they gave output that helps to measure PPD and PMV value.Envimet does not allow albedo to be changed. Rayman allows the albedo to be changed. After providing inputs(weather parameters, pavement properties in Envimets, outputs such as MRT and PET values were collected and used in Rayman as the inputs(Value of PET and MRT from Envimet, pavement properties with different values of albedo) which were required for the optimization process. A flowchart (figure 4.7) has been shown in chapter 4 (methodology, section 4.9)to state the interaction between Envimet and Rayman.

(iii)Can Envi-Met/RayMan predict the pavement temperature and other microclimate factors?

Envi-Met can predict factors like MRT,PET,Albedo and RayMan could optimize them

(iv)Can Envimet & RayMan measure and evaluate the human thermal comfort level for adults and children?Yes,they were successful in measuring and evaluating human thermal comfort by calculating the values of Percentage of thermal satisfaction and dissatisfaction.

(v)Can I know the height that is required from/for PET (physiological equivalent temperature) model?

The height was used as .2 to 10m as the default value of the software.

(vi)Is there an optimum albedo, or does it monotonically affect human thermal comfort ?

The current study that utilized the Rayman software to look at thermal comfort vs peak albedo to understand what peak albedo results in best thermal comfort. The results provided .15 value as the optimum albedo.

The results of the current study suggest that an albedo value of .15 is the optimum level for achieving the highest level of human thermal comfort in microclimate scenarios based on the current study inputs and outputs. This finding was based on the lowest level of predicted percentage of dissatisfaction observed when the albedo value was .15. In other words, the microclimate scenarios with an albedo value of .15 resulted in the least amount of thermal discomfort among the study participants. This information can be useful for designers and planners who are interested in creating outdoor spaces that promote human comfort and well-being.

5.12: Study limitations: The limited scope and use of software might be one of the limitation of the study time is another constraint .Future development of the software's are required for getting accurate results .For achieving accuracy of the study, multiple simulation scenarios were conducted for the study. Each simulation took around 5 hours to 12 hours to complete. For future development, the simulation time can be reduced through software improvement ,thus making the software faster.

Chapter 6: Summary, Conclusions and Recommendations

6.1 Summary and conclusions

Experimental sections were designed and constructed in EnviMet and Rayman, including asphalt pavement, and concrete pavement.The sections (with the other existing pavements)in the software were used to measure the fundamental materials properties, along with other values such as albedo, mean radiant temperature and physiological equivalent temperature. The results of which were presented in Chapter 5 are summarized here and in other sections following, respectively.

EnviMet was used to conduct the simulation of asphalt and concrete pavement and RayMan software was used to optimize albedo for pavement-based scenarios to improve human thermal comfort.

The study utilized Rayman software to determine the optimum albedo value for thermal comfort. Rayman used the values of MRT,PET ,Surface temperature ,other weather parameters along with the albedo values to calculate PPD. And thus with variation of albedo value, optimization value was achieved. The results demonstrated that optimizing albedo could provide an optimum value for thermal comfort, but the study has limitations as albedo solely might not impact on human thermal comfort. Additional factors such as mean radiant temperature, surface temperature, physiological equivalent temperature, and humidity must be considered to find their impact on human thermal comfort. Overall, the study highlights the importance of albedo in thermal comfort and the need for further research in this area to provide more accurate results.

Future software development can contribute towards supporting the current study findings and in calculating peak albedo values by incorporating new methodologies and procedures.

6.2. **Recommendations and possible application of the study:**

The study might offers numerous chances for pavement and applied climatology research. The provided thermal indices can characterize and quantify mean circumstances. Moreover, extremes like heat waves and other climatic and health problems from the perspective of human biometeorology can also be addressed through thermal indices. The model can generate data by using results from regional and global climate models to quantify bio-climate conditions for future scenarios.

With the limitations, the study tried to find the scope for optimizing albedo for improving human thermal comfort. The findings suggested .15 as the optimum albedo value at which highest level of thermal comfort have been achieved based on current study inputs and outputs. With future improvements, such as the scope to change albedo in Envimet will support the study to use for the comparison between experimental and modeling studies in teaching and human thermal comfort study.

References:

1.Leal Filho, W., Echevarria Icaza, L., Neht, A., Klavins, M., & Morgan, E. A. (2018). Coping with the effects of urban heat islands. A literature-based study on understanding urban heat vulnerability and the need for resilience in cities in a global climate change context. *Journal of Cleaner Production*, *171*, 1140-1149. https://doi.org/10.1016/j.jclepro.2017.10.086

2. Yang, L., Qian, F., Song, D., & Zheng, K. (2016). Research on urban heat-island effect. *Procedia Engineering*, *169*, 11-18. https://doi.org/10.1016/j.proeng.2016.10.002

3.Yue, W., Liu, X., Zhou, Y., & Liu, Y. (2019). Impacts of urban configuration on urban heat island: An empirical study in China mega-cities. *Science of The Total Environment*, *671*, 1036-1046. https://doi.org/10.1016/j.scitotenv.2019.03.421

4.Gago, E., Roldan, J., Pacheco-Torres, R., & Ordóñez, J. (2013). The city and urban heat islands: A review of strategies to mitigate adverse effects. *Renewable and Sustainable Energy Reviews*, *25*, 749-758. https://doi.org/10.1016/j.rser.2013.05.057

5.Peng, S., Piao, S., Ciais, P., Friedlingstein, P., Ottle, C., Bréon, F., Nan, H., Zhou, L., & Myneni, R. B. (2011). Surface urban heat island across 419 global big cities. *Environmental Science & Technology*, *46*(2), 696-703. https://doi.org/10.1021/es2030438

6.Gartland, L. M. (2012). *Heat islands: Understanding and mitigating heat in urban areas*. Routledge. https://www.routledge.com/Heat-Islands-Understanding-and-Mitigating-Heat-in-Urban-Areas/Gartland/p/book/9781849712989

7. Liu, H., & Weng, Q. (2007). Seasonal variations in the relationship between landscape pattern and land surface temperature in Indianapolis, USA. *Environmental Monitoring and Assessment*, *144*(1-3), 199-219. https://doi.org/10.1007/s10661-007-9979-5

8. Emmanuel, R. (2005). Thermal comfort implications of urbanization in a warm-humid city: The olombo metropolitan region (CMR), Sri Lanka. *Building and Environment*, *40*(12), 1591-1601. https://doi.org/10.1016/j.buildenv.2004.12.004

9.RIZWAN, A. M., DENNIS, L. Y., & LIU, C. (2008). A review on the generation, determination and mitigation of urban heat island. *Journal of Environmental Sciences*, *20*(1), 120-128. https://doi.org/10.1016/s1001-0742(08)60019-4

10. 2016v2 platform. (2023, January 23). US EPA. https://www.epa.gov/air-emissions-modeling/2016v2-platform

11. Dixon, P. G., & Mote, T. L. (2003). Patterns and causes of Atlanta's urban heat island–initiated precipitation. *Journal of Applied Meteorology*, *42*(9), 1273-1284. https://doi.org/10.1175/1520-0450(2003)042<1273:pacoau>2.0.co;2

12. Santamouris, M., Cartalis, C., Synnefa, A., & Kolokotsa, D. (2015). On the impact of urban heat island and global warming on the power demand and electricity consumption of buildings—A review. *Energy and Buildings*, *98*, 119-124. https://doi.org/10.1016/j.enbuild.2014.09.052

13.Hondula, D. M., & Barnett, A. G. (2014). Heat-related morbidity in Brisbane, Australia: Spatial variationnd area-level predictors. *Environmental Health Perspectives*, *122*(8), 831-836. https://doi.org/10.1289/ehp.1307496

14. Chow, W. T., Chuang, W., & Gober, P. (2012). Vulnerability to extreme heat in metropolitan Phoenix: Spatial, temporal, and demographic dimensions. *The Professional Geographer*, *64*(2), 286-302. https://doi.org/10.1080/00330124.2011.600225

15.Deilami, K., Kamruzzaman, M., & Liu, Y. (2018). Urban heat island effect: A systematic review of spatio-temporal factors, data, methods, and mitigation measures. *International Journal of Applied Earth Observation and Geo information*, *67*, 30-42. https://doi.org/10.1016/j.jag.2017.12.009

16.Zhang, K., Wang, R., Shen, C., & Da, L. (2009). Temporal and spatial characteristics of the urban heat island during rapid urbanization in Shanghai, China. *Environmental Monitoring and Assessment*, *169*(1-4), 101-112. https://doi.org/10.1007/s10661-009-1154-8

17. Mirzaei, P. A., & Haghighat, F. (2010). Approaches to study urban heat island – Abilities and limitations. *Building and Environment*, *45*(10), 2192-2201. https://doi.org/10.1016/j.buildenv.2010.04.001

18. Krayenhoff, E. S., & Voogt, J. A. (2007). A microscale three-dimensional urban energy balance model for studying surface temperatures. *Boundary-Layer Meteorology*, *123*(3), 433-461. https://doi.org/10.1007/s10546-006-9153-6

19. Kato, S., & Yamaguchi, Y. (2005). Analysis of urban heat-island effect using ASTER and ETM+ data: Separation of anthropogenic heat discharge and natural heat radiation from sensible heat flux. *Remote Sensing of Environment*, *99*(1-2), 44-54. https://doi.org/10.1016/j.rse.2005.04.026

20. NASA. (2018, January 1). *Land Surface Temperature Product Validation Best Practice Protocol. Version1.1*. https://www.researchgate.net/publication/327012239_Land_Surface_Temperature_Product_Validation_Best_Practice_Protocol_Version_11

21. Land Surface Temperature. (2017). In *Comprehensive remote sensing* (5th ed., pp. 264-283). Elsevier.

22. Shi, H., Xian, G., Auch, R., Gallo, K., & Zhou, Q. (2021). Urban heat island and its regional effects using remotely sensed thermal data—A review of recent developments and methodology. *Land*, *10*(8), 867. https://doi.org/10.3390/land10080867

23. Sheridan, S. C. (2011). *A spatial synoptic classification approach to projected heat vulnerability in California under future climate change scenarios*. California Air Resources Board and the California Environmental Protection
Agency. https://ww2.arb.ca.gov/sites/default/files/classic//research/apr/past/07-304.pdf

24. Akbari, H., Pomerantz, M., & Taha, H. (2001). Cool surfaces and shade trees to reduce energy use and improve air quality in urban areas. *Solar Energy*, *70*(3), 295-310. https://doi.org/10.1016/s0038-092x(00)00089-x

25. Akbari, H. (2005) Energy Saving Potentials and Air Quality Benefits of Urban Heat Island Mitigation (PDF) (19 pp, 251K). Lawrence Berkeley National Laboratory, Berkeley. http://heatisland.lbl.gov/

26. Sailor, D. J. 2002. Urban Heat Islands, Opportunities and Challenges for Mitigation and Adaptation. North American Urban Heat Island Summit. Toronto, Canada. 1-4 May 2002

27. Yamashita, Y., Sakamoto, K., Akiyoshi, H., Takahashi, M., Nagashima, T., & Zhou, L. B. (2010). Ozone and temperature response of a chemistry climate model to the solar cycle and sea surface temperature. *Journal of Geophysical Research*, *115*. https://doi.org/10.1029/2009jd013436

28. Pomerantz, M., Akbari, H., & Harvey, J. (2000). Cooler reflective pavements give benefits beyond energy savings: durability and illumination. *Lawrence Berkeley National Laboratory*. https://escholarship.org/uc/item/85f4j7pj

29. Chen, M. Z., Wei, W., & Wu, S. P. (2009). On cold materials of pavement and high-temperature performance of asphalt concrete. *Materials Science Forum*, *620-622*, 379-
382. https://doi.org/10.4028/www.scientific.net/msf.620-622.379

30. Nishizawa, T., Ozeki, T., Katoh, K., & Matsui, K. (2009). Finite element model analysis of thermal stresses of thick airport concrete pavement slabs. *Transportation Research Record: Journal of the Transportation Research Board*, *2095*(1), 3-12. https://doi.org/10.3141/2095-01

31. Johnston, D. P., & Surdahl, R. W. (2007). Influence of mixture design and environmental factors on continuously reinforced concrete pavement cracking. *Transportation Research Record: Journal of the Transportation Research Board*, *2020*(1), 83-88. https://doi.org/10.3141/2020-11

32. Hall, A., & Qu, X. (2006). Using the current seasonal cycle to constrain snow albedo feedback in future climate change. *Geophysical Research Letters*, *33*(3). https://doi.org/10.1029/2005gl025127

33.Kumar, V., Ranjan, D., & Verma, K. (2021). Global climate change. *Global Climate Change*, 187-
211. https://doi.org/10.1016/b978-0-12-822928-6.00002-2

34. Nikolopoulou, M., & Lykoudis, S. (2007). Use of outdoor spaces and microclimate in a Mediterranean urban area. *Building and Environment*, *42*(10), 3691-
3707. https://doi.org/10.1016/j.buildenv.2006.09.008

35. Wang, Y., & Akbari, H. (2016). The effects of street tree planting on urban heat island mitigation in Montreal. *Sustainable Cities and Society*, *27*, 122-128. https://doi.org/10.1016/j.scs.2016.04.013

36. Erell, E., Pearlmutter, D., Boneh, D., & Kutiel, P. B. (2014). Effect of high-albedo materials on pedestrian heat stress in urban street canyons. *Urban Climate*, *10*, 367-386. https://doi.org/10.1016/j.uclim.2013.10.005

37. Brunel University research archive: Impact of urban albedo on microclimate and thermal comfort over a heat wave event in London*. (2018, May 14). Brunel University Research Archive. https://bura.brunel.ac.uk/handle/2438/22214*

38. Lopez-Cabeza, V. P., Alzate-Gaviria, S., Diz-Mellado, E., Rivera-Gomez, C., & Galan-Marin, C. (2022). Albedo influences the microclimate and thermal comfort of courtyards under Mediterranean hot summer climate conditions. *Sustainable Cities and Society*, *81*, 103872. https://doi.org/10.1016/j.scs.2022.103872

39. Tian, L., Lin, Z., Liu, J., & Wang, Q. (2008). Numerical study of indoor air quality and thermal comfort under stratum ventilation. *Progress in Computational Fluid Dynamics, An International Journal*, *8*(7/8), 541. https://doi.org/10.1504/pcfd.2008.021333

40. Peeters, L., Dear, R. D., Hensen, J., & D'haeseleer, W. (2009). Thermal comfort in residential buildings: Comfort values and scales for building energy simulation. *Applied Energy*, *86*(5), 772-780. https://doi.org/10.1016/j.apenergy.2008.07.011

41. Youngmin Jun, Chung Hee Park, Shim, H., & Tae Jin Kang. (2009). Thermal comfort properties of wearing caps from various textiles. *Textile Research Journal*, *79*(2), 179-189. https://doi.org/10.1177/0040517508093444

42. Hitchings, R. (2009). Studying thermal comfort in context. *Building Research & Information*, *37*(1), 89-94. https://doi.org/10.1080/09613210802610753

43.. Schiller, G., Arens, E. A, Bauman, F., Benton, C., Fountain, M., & Doherty, T. (1988). A field study of thermal environments and comfort in office buildings. *UC Berkeley: Center for the Built Environment*. https://escholarship.org/uc/item/4km240x7

44. Becker, R., & Paciuk, M. (2009). Thermal comfort in residential buildings – Failure to predict by Standard Model. *Building and Environment*, *44*(5), 948-960. https://doi.org/10.1016/j.buildenv.2008.06.011

45.Streblow, R., et al., Evaluation of thermal comfort at inhomogeneous environmental conditions. Bauphysik, 2009. 31(1): p. 38-41. https://doi.org/10.1002/BAPI.200910006

46..Ribeiro, N.L., et al., Assessment of thermal comfort indexes, physiological limits, and thermal gradient of native sheep. Engenharia Agricola, 2008. 28(4): p. 614-623. https://doi.org/10.1590/S0100-69162008000400001

47. Lenzuni, P., Freda, D., & Del Gaudio, M. (2009). Classification of thermal environments for comfort assessment. *Annals of Occupational Hygiene*, *53*(4), 325-332. https://doi.org/10.1093/annhyg/mep012

48. Ho, S. H., Rosario, L., & Rahman, M. M. (2009). Three-dimensional analysis for hospital operating room thermal comfort and contaminant removal. *Applied Thermal Engineering*, *29*(10), 2080-2092. https://doi.org/10.1016/j.applthermaleng.2008.10.016

49. Hens, H. S. (2009). Thermal comfort in office buildings: Two case studies commented on. *Building and Environment*, *44*(7), 1399-1408. https://doi.org/10.1016/j.buildenv.2008.07.020

50. Catalina, T., Virgone, J., & Kuznik, F. (2009). Evaluation of thermal comfort using combined CFD and experimentation study in a test room equipped with a cooling ceiling. *Building and Environment*, *44*(8), 1740-1750. https://doi.org/10.1016/j.buildenv.2008.11.015

51. Yau, Y. H., & Chew, B. T. (2009). Thermal comfort study of hospital workers in Malaysia. *Indoor Air*, *19*(6), 500-510. https://doi.org/10.1111/j.1600-0668.2009.00617.x

52. Xu, X., Sit, K., Deng, S., & Chan, M. (2009). Thermal comfort in an office with intermittent air-conditioning operation. *Building Services Engineering Research and Technology*, *31*(1), 91-100. https://doi.org/10.1177/0143624409350118

53. Tseliou, A., Tsiros, I. X., Lykoudis, S., & Nikolopoulou, M. (2010). An evaluation of three bio meteorological indices for human thermal comfort in urban outdoor areas under real climatic conditions. *Building and Environment*, *45*(5), 1346-1352. https://doi.org/10.1016/j.buildenv.2009.11.009

54. Indraganti, M., & Rao, K. D. (2010). Effect of age, gender, economic group and tenure on thermal comfort: A field study in residential buildings in hot and dry climate with seasonal variations. *Energy and Buildings*, *42*(3), 273-281. https://doi.org/10.1016/j.enbuild.2009.09.003

55. Targhi, M. Z., & Van Dessel, S. (2015). Potential contribution of urban developments to outdoor thermal comfort conditions: The influence of urban geometry and form in Worcester, Massachusetts, USA. *Procedia Engineering*, *118*, 1153-1161. https://doi.org/10.1016/j.proeng.2015.08.457

56. Huttner, S., & Bruse, M. (2009). *Numerical modeling of the urban climate - a preview on ENVI-met 4.0*. ResearchGate. https://www.researchgate.net/publication/237757978_Numerical_modeling_of_the_urban_climate_-_a_preview_on_ENVI-met_40

57. Matzarakis, A., & Mayer, H. (1997). Heat stress in Greece. *International Journal of Biometeorology*, *41*(1), 34-39. https://doi.org/10.1007/s004840050051

58. *VDI 3789 - Environmental meteorology - Interactions between atmosphere and surfaces - Calculation of spectral short-wave and long-wave radiation*. (n.d.). VDI e.V. | VDI. https://www.vdi.de/en/home/vdi-standards/details/vdi-3789-environmental-meteorology-interactions-between-atmosphere-and-surfaces-calculation-of-spectral-short-wave-and-long-wave-radiation

59. *VDI 3787 Blatt 10 - Environmental meteorology - Human biometeorological requirements in the framework of recreation, prevention, therapy, and rehabilitation*.

60. *D. I. Verein, "VDI 3787, part I environmental meteorology, methods for the human-biometeorological evaluation of climate and air quality for the urban and regional planning at regional level. Part I climate," VDI/DIN-handbuch Reinhaltung Der Luft, band 1b, Dusseldorf, 1998, 29 P. - References - Scientific research publishing*. (n.d.). SCIRP Open Access. https://scirp.org/reference/referencespapers.aspx?referenceid=1076164

61. Gagge, A.P., Fobelets, A.P., & Berglund, L. (1986). A standard predictive index of human response to the thermal environment. *Ashrae Transactions, 92*, 709-731.https://www.aivc.org/sites/default/files/airbase_2522.pdf

62. Gagge, A.P., J. Stolwijk, and Y. Nishi, A (1971). standard predictive index of human response to the thermal environment. *ASHRAE Transactions*, 77(1): p. 247-262

63. Geng, W., & Heitzman, M. (2018). Measuring specific heat capacity of pavement materials. *Pavement Materials and Associated Geotechnical Aspects of Civil Infrastructures*, 126 135. https://doi.org/10.1007/978-3-319-95759-3_11

64. Hall, A., & Qu, X. (2006). Using the current seasonal cycle to constrain snow albedo feedback in future climate change. *Geophysical Research Letters*, *33*(3). https://doi.org/10.1029/2005gl025127

65. Höppe, P. (1999). The physiological equivalent temperature - a universal index for the biometeorological assessment of the thermal environment. *International Journal of Biometeorology*, *43*(2), 71-75. https://doi.org/10.1007/s004840050118

66. Li, H. (2016). Simulation of thermal behavior of design and management strategies for cool pavement. *Pavement Materials for Heat Island Mitigation*, 263-280. https://doi.org/10.1016/b978-0-12-803476-7.00012-x

67. *Standard 55 – Thermal environmental conditions for human occupancy*. (n.d.). ashrae.org. https://www.ashrae.org/technical-resources/bookstore/standard-55-thermal-environmental-conditions-for-human-occupancy

68. Matzarakis, A., Gangwisch, M., & Fröhlich, D. (2021). Rayman and SkyHelios model. *Urban Microclimate Modelling for Comfort and Energy Studies*, 339-361. https://doi.org/10.1007/978-3-030-65421-4_16

69. Liu, T., Liu, Z., Li, G., & Zuo, Z. (2015). Comparative study of numerical simulation of indoor thermal environment in the pattern of personalized ventilation and stratum ventilation. *Procedia Engineering*, *121*, 785-791. https://doi.org/10.1016/j.proeng.2015.09.031

70. Lin, Z., Tian, L., Yao, T., Wang, Q., & Chow, T. (2011). Experimental and numerical study of room airflow under stratum ventilation. Building and Environment, 46(1), 235-244. https://doi.org/10.1016/j.buildenv.2010.07.018

71. Sadeghian, P., Skredsvik, H., Baroni, M., Wang, C., & Sadrizadeh, S. (2021). Numerical study on the performance of the temperature-controlled airflow ventilation system during the movement of a patient from the operating room to the MRI room. *Building Simulation Conference Proceedings*. https://doi.org/10.26868/25222708.2021.30122

72. Shuter, B., & Aslani, A. (2000). Body surface area: Du bois and du bois revisited. *European Journal of Applied Physiology*, *82*(3), 250-254. https://doi.org/10.1007/s004210050679

73. International Organization for Standardization. (2004). (ISO Standard No. 8996). Ergonomics of the thermal environment — Determination of metabolic rate Retrieved From https://www.iso.org/obp/ui/#iso:std:iso:8996:ed-2:v1:en

74. Lin, T., Matzarakis, A., & Hwang, R. (2010). Shading effect on long-term outdoor thermal comfort. *Building and Environment*, *45*(1), 213-221. https://doi.org/10.1016/j.buildenv.2009.06.002

75. Lin, T., & Matzarakis, A. (2007). Tourism climate and thermal comfort in sun moon lake, Taiwan. *International Journal of Biometeorology*, *52*(4), 281-290. https://doi.org/10.1007/s00484-007-0122-7*inable Pavement Program - Sustainability - Pavements - Federal Highway Administration*. (n.d.). Www.fhwa.dot.gov. https://www.fhwa.dot.gov/pavement/sustainability/

76. Jeong, D., Park, K., & Song, B. (2016). A comparison between in-situ PET and ENVI-met PET for evaluating outdoor thermal comfort. *KIEAE Journal*, *16*(1), 11-19. https://doi.org/10.12813/kieae.2016.16.1.011

Appendix: The appendix consists tables and figures as a reference of Chapter 4 and 5 .Table AA1 TO AA10 shows the input values and A1 to A10, B1 to B10,C1 to C10 and D1 TO D10 denotes the output values of the simulation.

Table AA1: Showing the Temperature values from 21st June to 24th June with 72-hour period

Table AA2: Showing the Temperature values from July 15th to July 18th with 72-hour period.

Table AA3: Showing the Humidity values from 21st June to 24th June with 72-hour period

Table AA4: Showing the Humidity values from July 15th to July 18th with 72-hour period

Table AA5: Showing the Wind Speed values from June 21st June to June 24th with 72-hour period

Table AA6:: Showing the Wind Speed values from July 15th to July 18th with 72-hour period

Table AA7 to AA10: Showing the Surface Temperature values from July 15th to July 18th with 72 hour period

Table A1: Showing the MRT Values from June 21st to June 24th 2022with 72-hour period for asphalt zone

Table A2: Showing the Direct Radiation Values from 21st June to 24th June 2022with a 72-hour period for asphalt zone

Table A3: Showing the Reflected Radiation Values from 21st June to 24th June 2022 with 72-hour period for asphalt zone

Table A4 Showing the albedo Values from 21st June to 24th June 2022 with 72-hour period for asphalt zone

Table A5 5: Showing the PET (adult) values from 21st June to 24th June 2022 with 72-hour period for asphalt zone

Table A6: Showing the PET (Child) values from 21st June to 24th June 2022 with 72-hour period for asphalt zone

Table A7: Showing the PMV (Adult) values from 21st June to 24th June 2022 with 72-hour period for asphalt zone

Table A8: Showing the PMV (Child) values from 21st June to 24th June 2022 with 72-hour period for asphalt zone

Table A9: Showing the Percentage of satisfaction and dissatisfaction rate (DS) of adult from 21st June 2022 to 24th June 2022 with 72-hour period(asphalt)

Table A 10 : Showing the Percentage of satisfaction and dissatisfaction rate (DS) of child from 21st June 2022 to 24th June 2022 with 72-hour period(asphalt)

Table: B1 Showing the MRT Values from June 21st to June 24th 2022with 72-hour period for concrete zone

Table B2: Showing the Direct Radiation Values from 21st June to 24th June 2022with a 72-hour period for concrete zone.

Table B3: Showing the Reflected Radiation Values from 21st June to 24th June 2022 with 72-hour period for concrete zone

Table B4 Showing the albedo Values from 21st June to 24th June 2022 with 72-hour period for concrete zone

Table B5: Showing the PET (adult) values from 21st June to 24th June 2022 with 72-hour period for concrete zone

Table B6: Showing the PET (Child) values from 21st June to 24th June 2022 with 72-hour period for concrete zone

Table B7: Showing the PMV (Adult) values from 21st June to 24th June 2022 with 72-hour period for concrete zone

Table B8: Showing the PMV (Child) values from 21st June to 24th June 2022 with 72-hour period for concrete zone

Table B9: Showing the Percentage of satisfaction and dissatisfaction rate (DS) of adult from 21st June 2022 to 24th June 2022 with 72-hour period(concrete)

Table B10: Showing the Percentage of satisfaction and dissatisfaction rate (DS) of child from 21st June 2022 to 24th June 2022 with 72-hour period(concrete)

Table: C1 Showing the MRT Values from July 15th to July 18th 2022with 72-hour period for asphalt zone

Table C2: Showing the Direct Radiation Values from July 15th to July 18th 2022with a 72-hour period for asphalt zone

Table C3: Showing the Reflected Radiation Values from July15 th to July 18th 2022 with 72-hour period for asphalt zone

Table C4 Showing the albedo Values from July 1 th to July 18th July 2022 with 72-hour period for asphalt zone

Table C5: Showing the PET (adult) values from July 15th to July 18th 2022 with 72-hour period for asphalt zone

Table C6: Showing the PET (Child) values from July 15th to July 18th July 2022 with 72-hour period for asphalt zone

Table C7: Showing the PMV (Adult) values from July 15th to July 18th July 2022 with 72-hour period for asphalt zone

Table C8: Showing the PMV (Child) values from July 15th to July 18th July 2022 with 72-hour period for asphalt zone

Table C9: Showing the Percentage of satisfaction and dissatisfaction rate (DS) of adult from 15th July 2022 to 18th July 2022 with 72-hour period(asphalt)

Table C10: Showing the Percentage of satisfaction and dissatisfaction rate (DS) of adult from July 15th 2022 to July 18th 2022 with 72-hour period(asphalt)

Table: D1 Showing the MRT Values from July 15th to July 18th 2022with 72-hour period for concrete zone

Table D2: Showing the Direct Radiation Values from July 15th to July 18th 2022with a 72-hour period for concrete zone

Table D3: Showing the Reflected Radiation Values from July 15th to July 18th 2022 with 72-hour period for concrete zone

Table D4 Showing the albedo Values from July 15th to July 18th July 2022 with 72-hour period for concrete zone

Table D5: Showing the PET (adult) values from July 15th to July 18th 2022 with 72-hour period for concrete zone

Table D6: Showing the PET (Child) values from July 15th to July 18th July 2022 with 72-hour period for concrete zone

Table D7: Showing the PMV (Child) values from July 15th to July 18th July 2022 with 72-hour period for the concrete zone

Table D8: Showing the PMV (Adult) values from July 15th to July 18th July 2022 with 72-hour period for concrete zone

Table D9: Showing the Percentage of satisfaction and dissatisfaction (DS)rate of adult from July 15th 2022 to July 18th 2022 with 72-hour period(concrete)

Table D 10: Showing the Percentage of satisfaction and dissatisfaction rate (DS) of child from July 15th 2022 to July 18th 2022 with 72-hour period(concrete)

Appendix:

Table AA1:

Unit: Temperature in Degree Celsius

Time	21St June-22nd June	22nd June-23rd June	23rd June-23rd June 24th
9 am	26	26.1	27
10 am	30	28.8	30
11 am	33.88	30.5	31
12 pm	35.5	32.7	32.7
1 pm	36.6	35.5	33.8
2 pm	37.7	36.1	35.5
3 pm	38.8	36.1	36.1
4 pm	39.4	37.2	35.5
5 pm	40	37	35
6 pm	39.4	35	34.4
7 pm	39.4	32.2	33.3
8 pm	36.6	32.2	31.6
9 pm	32.7	28.8	29.4
10 pm	28.3	26.6	27.7
11 pm	25.5	23.8	28.3
12 pm	24.4	22.7	26.6
1 am	24.4	22.2	25.5
2 am	24	21.6	25.5
3 am	23.2	21.1	24
4 am	21.1	20	24.4
5 am	20	19.4	23.8
6 am	18.8	19	25
7 am	21.6	20	25
8 am	26.1	22.230	24.4

Table: AA-2

Air Temperature: asphalt/concrete

Time (Height:2m to 10m)	15th July -16th July Degree C	16th July-17th July Degree C	17th July-18th July Degree C
9 am	22.726.1	20	19.4
10 am	26.1	22.7	22.2
11 am	28.8	26.1	25.5
12 am	32.2	29.4	28.3
1 pm	34.4	33.27	30.5
2 pm	36.1	35	31
3 pm	37.7	37.2	33.8
4 pm	38.81	38.3	35
5 pm	39	38.5	35
6 pm	37.27	37	33.8
7 pm	33.8	37.2	31..6
8 pm	30.5	33.8	28.8
9 pm	27.7	30	26.1
10 pm	26.1	28.7	27.74
11 pm	27	26.1	21.6
12 am	23.8	24.4	20.5
1 am	22.7	22.2	19.4
2 am	22.7	21.6	18.8
3 am	21.6	21.1	17.7
4 am	21.6	20.5	17.2
5 am	20	19.4	17.2
6 am	20.1	18.8	16.6
7 am	19.4	16.1	16.1
8 am	20.5	17.2	17.2

Table AA-3: Humidity asphalt/concrete

Unit: Humidity Unit: in %

Time (Height:2m to 10m)	21St June-22nd June	22nd June-23rd June/	23rd June-24th June
9 am	30	32	42
10 am	23	28	35
11 am	17	26	30
12 pm	13	24	26
1 pm	11	22	21
2 pm	10	18	19
3 pm	9	19	19
4 pm	8	21	17
5 pm	8	22	18
6 pm	7	23	18
7 pm	8	27	24
8 pm	11	31	25
9 pm	16	28	30
10 pm	27	34	32
11 pm	39	32	40
12 pm	45	32	41
1 am	48	32	42
2 am	36	32	42
3 am	41	36	42
4 am	51	37	43
5 am	53	39	39
6 am	47	36	36
7 am	46	37	40
8 am	36	43	48

Table AA-4

Humidity unit in %

For asphalt/concrete

Time (Height:2m to 10m)	15th July -16th July (%)	16th July-17th July (%)	17th July-18th July (%)
9 am	66	63	55
10 am	57	55	45
11 am	46	47	38
12 pm	43	37	32
1 pm	37	30	30
2 pm	37	24	24
3 pm	29	16	21
4 pm	19	14	12
5 pm	23	14	12
6 pm	23	16	17
7 pm	30	12	25
8 pm	33	17	28
9 pm	39	32	32
10 pm	48	35	38
11 pm	55	38	43
12 am	57	43	40
1 am	61	52	44
2 am	63	51	46
3 am	68	53	49
4 am	70	55	49
5 am	73	61	57
6 am	73	63	57
7 am	78	63	59
8 am	75	59	51

Table AA-5

Wind Speed Unit: m/s for asphalt/concrete

Time (Height:2m to 10m)	21St June-22nd June	22nd June-23rd June/	23rd June-24th June
9 am	4	3.1	2.7
10 am	5.8	4	2.7
11 am	5.8	3.5	2.2
12 pm	4.4	3.5	2.2
1 pm	5.3645	3.5	-
2 pm	-	4.4	3.12
3 pm	4.4	5.81	2.2
4 pm	4.4	5.81	4.02
5 pm	4.4	2.7	4.02
6 pm	3.1293	2.7	4.4
7 pm	4.4	3.5	4.4
8 pm	3.12	3.5	5.3
9 pm	2.68	5.3	2.7
10 pm	-	4.4	2.7
11 pm	-	-	2.7
12 pm	1.34	2.21	2.2
1 am	-	2.7	2.2
2 am	1.34	1.34	2.2
3 am	2.23	3.5	2.2
4 am	-	4.2	2.2
5 am	3.12	3.12	2.2
6 am	-	3.12	2.2
7 am	2.23	2.7	1.34
8 am	2.21	3.12	3.12

*- Denotes the wind speed as calm (close to 0)

Table AA-6

Wind Speed: **asphalt/concrete**

Time (Height:2m to 10m)	15th July -16th July (m/s)	16th July-17th July(m/s)	17th July-18th July(m/s)
9 am	3.12	-	3.12
10 am	2.2	1.34	3.12
11 am	2.7	2.2	2.7
12 am	3.5	1.34	3.5
1 pm	2.7	2.7	3.12
2 pm	2.2	2.7	3.5
3 pm	2.7	2.2	3.5
4 pm	3.12	1.7	5.8
5 pm	3.12	2.2	6.2
6 pm	4.02	3.12	4.4
7 pm	3.5	4.4	4.4
8 pm	3.5	3.12	4.4
9 pm	3.12	3.12	3.5
10 pm	3.12	2.2	5.3
11 pm	3.12	3.12	1.34
12 am	1.34	3.12	3.12
1 am	2.2	2.7	2.2
2 am	-	2.2	2.7
3 am	1.34	2.2	-
4 am	1.34	2.2	2.7
5 am	2.2	1.34	2.2

*- Denotes the wind speed as calm (close to 0)

Table: AA-7

Surface temperature of asphalt for June 21st June to June 24th

Unit:Degree Celsius

Time (Height:2m to 10m)	21st June-22nd june	22nd june-23rd june	23rd June-24th june
9:00 am	48	49	50
10:00 am	55	57	58
11:00 am	61	62	63
12:00 pm	64	65	66
1:00 pm	66	67	68
2:00 pm	68	69	70
3:00 pm	70	71	72
4:00 pm	71	72	73
5:00 pm	72	73	74
6:00 pm	71	73	75
7:00 pm	71	73	76
8:00 pm	66	67	68
9:00 pm	60	62	63
10:00 pm	52	53	54
11:00 pm	47	48	49
12:00 pm	45	47	49
1:00 am	45	47	48
2:00 am	45	46	47
3:00 am	43	45	46
4:00 am	40	41	42
5:00 am	38	39	40
6:00 am	36	37	42
7:00 am	41	42	43
8:00 am	48	49	50

Table AA-7: Surface temperature of asphalt for June 21st June to June 24th

Table AA-8:

Surface temperature of asphalt for June 21st June to June 24th

Unit:Degree Celsius

Time (Height:2m to 10m)	21st June-22nd June	22nd june-23rd June	23rd June-24th June
9:00 am	28	28	30
10:00 am	42	41	43
11:00 am	55	52	54
12:00 pm	61	58	60
1:00 pm	65	63	65
2:00 pm	68	67	68
3:00 pm	72	68	69
4:00 pm	74	71	72
5:00 pm	76	72	73
6:00 pm	74	70	72
7:00 pm	74	70	72
8:00 pm	65	63	65
9:00 pm	52	48	51
10:00 pm	36	35	37
11:00 pm	26	25	27
12:00 pm	23	21	23
1:00 am	23	21	23
2:00 am	21	20	22
3:00 am	19	18	21
4:00 am	11	10	11
5:00 am	8	7	9
6:00 am	20	18	21
7:00 am	23	21	23
8:00 am	28	25	28

Table AA-8: Surface temperature of concrete for June 21st June to June 24th

Table AA-9:

Surface temperature of asphalt for July 15th to July 18th

Unit:Degree Celsius

Time (Height:2m to 10m)	15-16th July	16-17th July	17-18th July
9:00 am	42	39	39
10:00 am	48	46	46
11:00 am	53	51	50
12:00 pm	59	56	55
1:00 pm	62	61	60
2:00 pm	65	64	63
3:00 pm	67	64	63
4:00 pm	69	67	66
5:00 pm	70	68	67
6:00 pm	67	69	68
7:00 pm	60	58	57
8:00 pm	56	54	53
9:00 pm	51	49	48
10:00 pm	48	47	46
11:00 pm	50	47	47
12:00 pm	44	41	40
1:00 am	42	39	37
2:00 am	42	38	36
3:00 am	41	38	37
4:00 am	41	37	36
5:00 am	41	38	37
6:00 am	38	36	35
7:00 am	37	35	34
8:00 am	39	38	37

Table AA-9: Surface temperature of asphalt for July 15th to July 18th

Table AA-10:

Surface temperature of concrete for July 15th to July 18th

Unit:Degree Celsius

Time (Height:2m to 10m)	15-16th July	16-17th July	17-18th July
9:00 am	17	16	16
10:00 am	29	28	27
11:00 am	38	37	36
12:00 pm	49	47	46
1:00 pm	56	55	54
2:00 pm	63	62	61
3:00 pm	68	66	65
4:00 pm	72	71	70
5:00 pm	73	72	71
6:00 pm	67	65	64
7:00 pm	55	54	53
8:00 pm	44	43	42
9:00 pm	34	33	32
10:00 pm	29	28	27
11:00 pm	32	31	30
12:00 pm	21	20	19
1:00 am	17	16	15
2:00 am	17	16	15
3:00 am	13	12	11
4:00 am	13	12	11
5:00 am	8	7	7
6:00 am	8	7	6
7:00 am	7	7	6
8:00 am	20	19	17

Table AA-10: Surface temperature of concrete for July 15th to July 18th

Scenario A For Asphalt pavement region,21st June to 24th June 2022

(Note: Table A-1 to Table A-10 are the output from Envimet.Table A-11 is the output from Rayman.)

Table A-1

MRT Values: MRT values for the time 21st June,9:00 am to 24th June 9: have been plotted. We can see the variation of values hereby in the table. The values increase in the early morning to reach peak value at 4 pm and start to decrease after that and reach lowest value at mid night.

Time	21St June-22nd June (Degree C)	22nd June-23rd June (Degree C)	23rd June-24th June (Degree C)
9:00 am	59.72	61.41	61,56
10:00 am	62,15	62.15	62,28
11:00 am	63.16	63.16	63,27
12:00 pm	65.73	65.83	65,88
1:00 pm	68.77	68.77	68,87
2:00 pm	70.96	70.96	71,05
3:00 pm	71.53	71.53	71,63
4:00 pm	67.5	67.5	67,62
5:00 pm	58.48	58.48	58,62
6:00 pm	35.8	35.8	36,04
7:00 pm	29.71	29.71	29,87
8:00 pm	27.72	27.72	27,88
9:00 pm	25.87	25.87	26,03
10:00 pm	24.08	24.08	24,24
11:00 pm	22.32	22.32	22,48
12:00 am	20.58	20.58	20,74
1:00 am	18.36	18.86	19,02
2:00 am	17.5	17.5	17,3
3:00 am	15.45	15.45	15,59
4:00 am	13.75	13.75	13,9
5:00 am	36.98	36.98	37,09
6:00 am	49.48	49.48	49,45
7:00 am	56.08	56.08	56,14
8:00 am	59.86	59.86	59,92

Table A-2 (For Asphalt pavement region)

Direct Radiation:

Direct radiation is also sometimes called "beam radiation" or "direct beam radiation". It is used to describe solar radiation traveling on a straight line from the sundown to the surface of the earth.

Time	21St June-22nd June(W/m^2)	22nd June-23rd June(W/m^2)	23rd June-24th June(W/m^2)
9 am	1028	1028	1028
10 am	1050	1050	1049
11 am	1059	1059	1058
12 pm	1056	1056	1056
1 pm	1042	1042	1042
2 pm	1013	1013	1013
3 pm	961	961	961
4 pm	985.4	854	854
5 pm	644	645	645
6 pm	81	83	83
7 pm	1	1	1
8 pm	1	1	1
9 pm	1	1	1
10 pm	1	1	1
11 pm	1	1	1
12 pm	1	1	1
1 am	1	1	1
2 am	1	1	1
3 am	1	1	1
4 am	1	1	1
5 am	533	532	530
6 am	794	794	793
7 am	918	918	918
8 am	981	986	986

Table A-3 (For Asphalt pavement region)

Reflected Radiation:

Reflected radiation describes sunlight that has been reflected off non-atmospheric things such as the ground.

Time	21St June-22nd June W/m^2)	22nd June-23rd June W/m^2)	23rd June-24th June W/m^2)
9 am	196.91	196.71	197
10 am	220	220	221.5
11 am	230.80	230.80	231
12 pm	228.647	228.5	229
1 pm	213.24	213.25	214
2 pm	186.24	186.3	186.5
3 pm	149.26	149.27	149.27
4 pm	163.99	162	162
5 pm	55	72	55.31
6 pm	9	8	9
7 pm	1	1	1
8 pm	1	1	1
9 pm	1	1	1
10 pm	1	1	1
11 pm	1	1	1
12 pm	1	1	1
1 am	1	1	1
2 am	1	1	1
3 am	1	1	1
4 am	1	1	1
5 am	25.46	25.05	25.45
6 am	73.05	72.63	73
7 am	120.27	119.88	120.21
8 am	162.53	162.19	163.21

Table A-3: Showing the Reflected Radiation Values from 21st June to 24th June with 72-hour period.

Table A-4 (For asphalt pavement region)

Albedo Values :

(Found by dividing reflected radiation to direct radiation)

The following table shows Albedo values collected from EnviMet/RayMan simulation for the time 21st June,9:00 am to 24th June 9: have been plotted. We can see the variation of values hereby in the table. The values increase in the early morning to reach peak value around 5 pm.

Time	21St June-22nd June	22nd June-23rd June	23rd June-24th June
9 am	.191	.192	.192
10 am	.21	.21	.21
11 am	.217	.215	.217
12 pm	.214	.20	.214
1 pm	.20	.182	.20
2 pm	.183	.154	.182
3 pm	.155	.24	.155
4 pm	.120	.12	.12
5 pm	.24	.242	.24
6 pm	.11	.12	.12
7 pm	1	1	1
8 pm	1	1	1
9 pm	1	1	1
10 pm	1	1	1
11 pm	1	1	1
12 pm	1	1	1
1 am	1	1	1
2 am	1	1	1
3 am	1	1	1
4 am	1	1	1
5 am	.04	.041	.042
6 am	.09	.092	.093
7 am	.13	.131	.132
8 am	.165	.1652	.1653

Table A-5 (For asphalt pavement region)

PET(Adult): (Asphalt) The following table shows PET values for the time 21st June,9:00 am to 24th June 9: have been plotted. We can see the variation of values hereby in the table. The values increase in the early morning to reach peak value around 5 pm.

Time	21St June-22nd June (Temp in Degree C)	22nd June-23rd June (Temp in Degree C)	23rd June-24th June (Temp in Degree C)
9 am	13.3	13.6	13.6
10 am	18.9	18.8	18.9
11 am	23.6	23.7	23.8
12 pm	30.5	30.2	30.4
1 pm	32	33	33.2
2 pm	33	33.4	33.5
3 pm	33.5	33.5	33.6
4 pm	34.5	34.7	34.8
5 pm	34.6	34.8	35
6 pm	34.4	34.9	34.1
7 pm	32	32.4	33
8 pm	31	31.4	32,2
9 pm	21.8	21.9	22.3
10 pm	20	20.4	20.6
11 pm	19	19.5	19.7
12 pm	19	19.4	19.7
1 am	18	18.5	18.8
2 am	17.5	17.6	17.9
3 am	16	16.4	17.1
4 am	17	17.4	18.1
5 am	17.5	17.6	18.2
6 am	19	19.6	20.1
7 am	20	20.6	20.8
8 am	22	22.4	22.6

Table A-6 **(For asphalt pavement region)**

PET(Child)

The following table shows PET values for the time 21st June,9:00 am to 24th June 9: have been plotted. We can see the variation of values hereby in the table. The values increase in the early morning to reach peak value around 6 pm.

Time	21St June-22nd June (Temp in Degree C)	22nd June-23rd June (Temp in Degree C)	23rd June-24th June (Temp in Degree C)
9 am	13.5	13.8	14.1
10 am	19.1	18.9	19.2
11 am	23.7	23.9	24.2
12 pm	30.6	30.8	31.4
1 pm	32.1	32.5	33.7
2 pm	33.4	33.9	34
3 pm	33.9	33.8	34.1
4 pm	34.8	34.9	35.1
5 pm	34.9	35.2	36
6 pm	34.7	35.3	34.6
7 pm	32.4	33	33.4
8 pm	31.4	31.8	32,7
9 pm	21.9	22.4	22.8
10 pm	20.5	20.9	20.8
11 pm	19.4	20.1	20.4
12 pm	19.9	19.7	20.2
1 am	18.4	19.1	20.3
2 am	17.7	18.2	18.5
3 am	16.8	17.2	17.6
4 am	17.5	18.2	18.4
5 am	17.9	18.4	18.8
6 am	19.2	20.3	20.9
7 am	20.5	20.9	21.3
8 am	22.8	22.8	22.9

Table A-7 **(For asphalt pavement region)**

PMV (Adult) The following table shows PMV values for the time 21st June,9:00 am to 24th June 9: have been plotted. We can see the variation of values hereby in the table. The values increase in the early morning to reach peak value around 5 pm.

Unit: None (Unit less)

Time	21St June-22nd June	22nd June-23rd June	23rd June-24th June
9 am	1.15	1.51	1.51
10 am	1.52	1.53	1.57
11 am	1.83	1.85	1.87
12 pm	2.2	2.25	2.27
1 pm	2.37	2.41	2.43
2 pm	2.42	2.42	2.44
3 pm	2.5	2.51	2.54
4 pm	2.54	2.55	2.56
5 pm	2.54	2.55	2.59
6 pm	2.55	2.57	2.59
7 pm	2.37	2.41	2.43
8 pm	2.31	2.33	2.37
9 pm	1.71	1.72	1.75
10 pm	1.60	1.62	1.66
11 pm	1.53	1.55	1.59
12 pm	1.53	1.54	1.58
1 am	1.46	1.48	1.53
2 am	1.43	1.46	1.51
3 am	1..33	1.35	1.41
4 am	1.4	1.42	1.46
5 am	1.432	1.45	1.51
6 am	1.53	1.55	1.62
7 am	1.59	1.61	1.64
8 am	1.72	1.73	1.77

Table A-8 **(For asphalt pavement region)**

PMV (Child)

The following table shows PMV values for the time 21st June,9:00 am to 24th June 9: have been plotted. We can see the variation of values hereby in the table. The values increase in the early morning to reach peak value around 5 pm.

Unit: None

Time	21St June-22nd June	22nd June-23rd June	23rd June-24th June
9 am	1.17	1.5	1.52
10 am	1.53	1.54	1.58
11 am	1.83	1.85	1.91
12 pm	2.2	2.4	2.47
1 pm	2.38	2.42	2.47
2 pm	2.46	2.53	2.58
3 pm	2.50	2.55	2.59
4 pm	2.56	2.62	2.66
5 pm	2.57	2.62	2.66
6 pm	2.55	2.59	2.63
7 pm	2.40	2.45	2.49
8 pm	2.33	2.39	2.45
9 pm	1.71	1.76	1.82
10 pm	1.62	1.67	1.72
11 pm	1.55	1.58	1.63
12 pm	1.58	1.62	1.67
1 am	1.49	1.55	1.59
2 am	1.44	1.48	1.53
3 am	1.38	1.42	1.47
4 am	1.43	1.47	1.52
5 am	1.45	1.48	1.54
6 am	1.54	1.58	1.63
7 am	1.62	1.66	1.72
8 am	1.77	1.81	1.86

Table A-9 **(For asphalt pavement region)**

Percentage of Satisfaction rate (Adult)

The following table shows Human Thermal Comfort (Adult) values for the time 21st June,9:00 am to 24th June 9: have been plotted. We can see the variation of values hereby in the table. The satisfaction values decrease after 9 am morning to reach a peak value around 6 pm and start to increase after that and reach the highest value between midnight to early morning.

Time	21St June-22nd June	22nd June-23rd June	23rd June-24th June
9 am	40	35	35
10 am	35	35	36
11 am	29	28	26
12 pm	22	25	23
1 pm	19	21	21
2 pm	17.5	18	20
3 pm	16	15	17
4 pm	15	14	13
5 pm	15	14	13
6 pm	15	14	13
7 pm	18.5	15	14
8 pm	20	18	14
9 pm	31.5	26	24
10 pm	34	29	25
11 pm	35	31	26
12 am	35	32	28
1 am	37	33	31
2 am	37	33	31
3 am	39	35	33
4 am	38	35	33
5 am	37	35	33
6 am	35	34	34
7 am	34	32	32
8 am	32	31	30

Table A-9: Showing the Percentage of satisfaction of adult from 21st June 2022 to 24th June 2022 with 72-hour period(asphalt)

Table A-10 **(For asphalt pavement region)**

Percentage of Satisfaction and dissatisfaction rate (Child)

The following table shows Human Thermal Comfort (Child) values for the time 21st June,9:00 am to 24th June 9: have been plotted. We can see the variation of values hereby in the table. The satisfaction values decrease after 9 am morning to reach a peak value around 6 pm and start to increase after that and reach the lowest highest value between midnight to early morning.

Time	21St June-22nd June	22nd June-23rd June	23rd June-24th June
9 am	42	34	34
10 am	35	33	35
11 am	29	27	26
12 pm	22	21	20
1 pm	19	18	17
2 pm	16.5	15	15
3 pm	16	15	15
4 pm	14.5	13	14
5 pm	13.5	13	14
6 pm	13	12	13
7 pm	18	17	16
8 pm	20	18	17
9 pm	31.5	29	27
10 pm	33	31	27
11 pm	35	33	28
12 am	35	33	29
1 am	36	34	29
2 am	37	35	33
3 am	38	36	34
4 am	37	37	35
5 am	36.5	34	35
6 am	35	33	32
7 am	33.2	32	31
8 am	31.3	31	30

Table A-10: Showing the Percentage of satisfaction rate of child from 21st June 2022 to 24th June 2022 with 72-hour period(asphalt)

Note:The ratio of body mass to surface area, also known as body surface area, can impact the amount of heat transfer between the body and the surrounding environment. Children generally have a larger body surface area relative to their mass, compared to adults, meaning that they are more susceptible to heat transfer and may feel more discomfort in hot environments. In addition to body surface area, other factors such as clothing, activity level, and personal tolerance for heat can also impact an individual's level of discomfort in a given environment. It is important to consider all of these factors when evaluating comfort levels for different populations.

Scenario B (For oncrete pavement region,21st June to 24th June 2022)

(Note:Table B-1 to Table B-10 are the output from Envimet.Table B-11 is the output from Rayman.)

Table B-1

MRT Values: For Concrete Pavement Region,21st June to 24th June 2022

MRT values for the time 21st June,9:00 am to 24th June 8:59 am have been plotted. We can see the variation of values hereby in the table. The values increase in the early morning to reach peak value at 4 pm and start to decrease after that and reach lowest value at mid night.

Time	21St June-22nd June (Degree C)	22nd June-23rd June (Degree C)	23rd June-24th June (Degree C)
9 am	59.1	59	58.9
10 am	62.	61.15	60.67
11 am	63.1	62.16	61.23
12 pm	65.3	65.43	65.23
1 pm	68.27	68.37	68.2
2 pm	70.2	69.46	71.12
3 pm	70.8	70.53	71.11
4 pm	66.49	66.50	65.23
5 pm	57	56.38	57.65
6 pm	34.80	33.20	33.10
7 pm	28.71	28.51	27.85
8 pm	27.22	27.32	27.12
9 pm	25.27	25.17	25.12
10 pm	23.88	23.18	23.1
11 pm	21.42	20.22	21.48
12 pm	20.58	20.14	20.44
1 am	17.36	17.12	18.82
2 am	17.2	17.12	16.30
3 am	15.35	14.32	15.49
4 am	12.35	12.21	13.50
5 am	35.98	34.78	37.09
6 am	48.48	47.9	49.,35
7 am	55.08	54.92	56.-5
8 am	58.62	57.78	58.92

Table B-2 (For concrete pavement region,21st June to 24th June 2022)

Direct Radiation

The following table shows Direct Radiation values from Envi-Met for the time 21st June,9:00 am to 24th June 8:59: have been plotted. We can see the variation of values hereby in the table. The values increase in the early morning to reach peak value at 12 pm.

Time	21St June-22nd June(W/m^2)	22nd June-23rd June(W/m^2)	23rd June-24th June(W/m^2)
9 am	1028	1028	1028
10 am	1050	1050	1049
11 am	1059	1059	1058
12 pm	1056	1056	1056
1 pm	1042	1042	1042
2 pm	1013	1013	1013
3 pm	961	961	961
4 pm	985.4	854	854
5 pm	644	645	645
6 pm	81	83	83
7 pm	1	1	1
8 pm	1	1	1
9 pm	1	1	1
10 pm	1	1	1
11 pm	1	1	1
12 pm	1	1	1
1 am	1	1	1
2 am	1	1	1
3 am	1	1	1
4 am	1	1	1
5 am	533	532	530
6 am	794	794	793
7 am	918	918	918
8 am	981	986	986

Table B-3:(For concrete pavement region,21st June to 24th June 2022)

Reflected Radiation Values from 21st June to 24th June with 72-hour period

	21St June-22nd June W/m^2)	22nd June-23rd June W/m^2)	23rd June-24th June W/m^2)
9 am	196.91	196.71	197
10 am	220	220	221.5
11 am	230.80	230.80	231
12 pm	228.647	228.5	229
1 pm	213.24	213.25	214
2 pm	186.24	186.3	186.5
3 pm	149.26	149.27	149.27
4 pm	163.99	162	162
5 pm	55	72	55.31
6 pm	9	8	9
7 pm	1	1	1
8 pm	1	1	1
9 pm	1	1	1
10 pm	1	1	1
11 pm	1	1	1
12 pm	1	1	1
1 am	1	1	1
2 am	1	1	1
3 am	1	1	1
4 am	1	1	1
5 am	25.46	25.05	25.45
6 am	73.05	72.63	73
7 am	120.27	119.88	120.21
8 am	162.53	162.19	163.21

Table B-4 (For concrete pavement region,21st June to 24th June 2022)

Albedo Values (Found by dividing reflected radiation to direct radiation)

The following table shows Albedo values collected from EnviMet/RayMan simulation for the time 21st June,9:00 am to 24th June 9: have been plotted. We can see the variation of values hereby in the table. The values increase in the early morning to reach peak value around 5 pm.

Time	21St June-22nd June	22nd June-23rd June	23rd June-24th June
9 am	.191	.192	.192
10 am	.21	.21	.21
11 am	.217	.215	.217
12 pm	.214	.20	.214
1 pm	.20	.182	.20
2 pm	.183	.154	.182
3 pm	.155	.24	.155
4 pm	.120	.12	.12
5 pm	.24	.242	.24
6 pm	.11	.12	.12
7 pm	1	1	1
8 pm	1	1	1
9 pm	1	1	1
10 pm	1	1	1
11 pm	1	1	1
12 pm	1	1	1
1 am	1	1	1
2 am	1	1	1
3 am	1	1	1
4 am	1	1	1
5 am	.04	.041	.042
6 am	.09	.092	.093
7 am	.13	.131	.132
8 am	.165	.1652	.1653

Table B-5 (For concrete pavement region,21st June to 24th June 2022)

PET(Adult)

The following table shows PET values for the time 21st June,9:00 am to 24th June 8:59 have been plotted. We can see the variation of values hereby in the table. The values increase in the early morning to reach peak value around 5 pm

Time	21St June-22nd June (Temp in Degree C)	22nd June-23rd June (Temp in Degree C)	23rd June-24th June (Temp in Degree C)
9 am	13.2	13.4	13.3
10 am	18.	18.5	18.5
11 am	23.5	23.2	23.5
12 pm	30.5	30.1	30.3
1 pm	32	32.8	33.1
2 pm	33	33.1	33.4
3 pm	33.3	33.2	33.5
4 pm	34.2	34.4	34.3
5 pm	34.3	34.5	34.8
6 pm	34.2	34.7	33.9
7 pm	32	32.3	32.6
8 pm	30.8	31.2	32,1
9 pm	21.5	21.5	22.2
10 pm	19.8	20.3	20.34
11 pm	19	19.4	19.5
12 pm	18.7	19.2	19.3
1 am	18	18.34	18.5
2 am	17.3	17.2	17.5
3 am	15.9	16.3	17.0
4 am	17	17.12	17.9
5 am	17.3	17.4	17.8
6 am	18.8	19.2	19.8
7 am	19.7	20.3	20.6
8 am	21.8	22.2	22.1

Table B-6 (For concrete pavement region,21st June to 24th June 2022)

PET(Child)

The following table shows PET values for the time 21st June,9:00 am to 24th June 8:59 have been plotted. We can see the variation of values hereby in the table. The values increase in the early morning to reach peak value around 6 pm

Time	21St June-22nd June (Temp in Degree C)	22nd June-23rd June (Temp in Degree C)	23rd June-24th June (Temp in Degree C)
9 am	13.3	13.5	14.0
10 am	19.0	18.9	19.1
11 am	23.4	23.4	24.7
12 pm	30.23	30.5	31.3
1 pm	32.2	32.3	33.4
2 pm	33.1	33.6	33.8
3 pm	33.4	33.6	33.9
4 pm	34.5	34.6	35.1
5 pm	34.9	35.1	35.8
6 pm	34.9	35.3	34.4
7 pm	32.6	33	33.3
8 pm	31.6	30.8	32,5
9 pm	22.6	22.3	22.3
10 pm	21	20.6	20.5
11 pm	19.3	19.6	20.2
12 pm	19.2	19.3	20.1
1 am	18.1	18.6	19.8
2 am	17.5	18.4	18.43
3 am	16.4	17.2	17.2
4 am	17.4	18.1	18.3
5 am	17.1	18.3	18.5
6 am	19.6	20.1	20.7
7 am	20.7	20.4	21.2
8 am	22.9	22.5	22.4

Table B-7: (For concrete pavement region,21st June to 24th June 2022)

PMV (Adult) The following table shows PMV values for the time 21st June,9:00 am to 24th June 8: 59 have been plotted. We can see the variation of values hereby in the table. The values increase in the early morning to reach peak value around 6 pm.

PMV (Adult): No unit

Time	21St June-22nd June	22nd June-23rd June	23rd June-24th June
9 am	1.12	1.11	1.16
10 am	1.54	1.52	1.54
11 am	1.84	1.81	1.85
12 pm	2.3	2.21	2.24
1 pm	2.29	2.38	2.42
2 pm	2.41	2.41	2.42
3 pm	2.5	2.48	2.53
4 pm	2.52	2.51	2.52
5 pm	2.52	2.52	2.54
6 pm	2.52	2.52	2.54
7 pm	2.34	2.40	2.41
8 pm	2.29	2.31	2.33
9 pm	1.70	1.69	1.74
10 pm	1.59	1.61	1.64
11 pm	1.48	1.52	1.53
12 pm	1.48	1.52	1.54
1 am	1.43	1.46	1.52
2 am	1.41	1.43	1.50
3 am	1..32	1.32	1.39
4 am	1.38	1.41	1.45
5 am	1.431	1.44	1.50
6 am	1.51	1.52	1.58
7 am	1.56	1.60	1.62
8 am	1.68	1.71	1.75

Table B-8: (For concrete pavement region,21st June to 24th June 2022)

PMV (Child)

The following table shows PMV values for the time 21st June,9:00 am to 24th June 9: have been plotted. We can see the variation of values hereby in the table. The values increase in the early morning to reach peak value around 6 pm

PMV (Child): No Unit

Time	21St June-22nd June	22nd June-23rd June	23rd June-24th June
9 am	1.14	1.21	1.18
10 am	1.52	1.54	1.55
11 am	1.79	1.83	1.90
12 pm	2.19	2.2	2.44
1 pm	2.35	2.40	2.45
2 pm	2.44	2.49	2.55
3 pm	2.49	2.51	2.56
4 pm	2.48	2.60	2.64
5 pm	2.53	2.61	2.63
6 pm	2.53	2.55	2.61
7 pm	2.39	2.432	2.48
8 pm	2.32	2.34	2.42
9 pm	1.68	1.75	1.78
10 pm	1.61	1.64	1.68
11 pm	1.53	1.56	1.61
12 pm	1.56	1.60	1.65
1 am	1.46	1.54	1.55
2 am	1.43	1.47	1.52
3 am	1.35	1.44	1.44
4 am	1.42	1.45	1.51
5 am	1.41	1.46	1.53
6 am	1.52	1.56	1.62
7 am	1.60	1.65	1.71
8 am	1.74	1.78	1.82

Table B-9 (For concrete pavement region,21st June to 24th June 2022)

Percentage of Satisfaction rate (Adult)

The following table shows Human Thermal Comfort (Adult) values for the time 21st June,9:00 am to 24th June 8:59 that have been plotted. We can see the variation of values hereby in the table. The satisfaction values decrease in the after 9 am morning to reach a peak value around 6 pm

Time	21St June-22nd June	22nd June-23rd June	23rd June-24th June
9 am	42	32	37
10 am	36	31	30
11 am	29	29	27
12 pm	22	25	22)
1 pm	19	22	20
2 pm	18	17	19
3 pm	16	14	18
4 pm	15	14	12
5 pm	16	13	12
6 pm	15	13	12
7 pm	18.5	15	13
8 pm	21	18	11
9 pm	32.5	24	22
10 pm	34.5	31	23
11 pm	35.6	34	25
12 am	35.5	35	29
1 am	37.4	37	32
2 am	37.7	38	34
3 am	39.8	38	35
4 am	38.5	39	35
5 am	37.7	40	36
6 am	35.5	42	37
7 am	34.4	39	33
8 am	32.6	38	30

Table B-9: Showing the Percentage of satisfaction rate of adult from 21st June 2022 to June 24th, 2022, 72-hour period(concrete)

Table B-10(For concrete pavement region,21st June to 24th June 2022)

Percentage of Satisfaction rate (Child)

The following table shows Human Thermal Comfort (Child) values for the time 21st June,9:00 am to 24th June 8:59am have been plotted. We can see the variation of values hereby in the table. The values decrease in the after 9 am morning to reach a peak value around 6 pm and start to increase after that and reach the lowest highest value between midnight to early morning.

Time	21St June-22nd June	22nd June-23rd June	23rd June-24th June
9 am	41	31	31
10 am	34	30	30
11 am	28	26	25
12 pm	22	24	29
1 pm	17	22	16
2 pm	15.5	21	15
3 pm	15	20	15
4 pm	14.5	20	15
5 pm	13.5	19	14
6 pm	12	18	13
7 pm	17	18	13
8 pm	21.9	21	16
9 pm	30.5	25	27
10 pm	33	29	28
11 pm	34	32	26
12 am	34	35	29
1 am	36	36	31
2 am	36	37	35
3 am	37	39	36
4 am	38	39	38
5 am	38.5	41	39
6 am	39	41	41
7 am	33.2	38	36
8 am	32.3	35	34

Scenario C: (For asphalt pavement region,15 July to 18th July 2022)

(Note:Table C-1 to Table C-10 are the output from Envimet,Table C-11 is the output from Rayman.)

Table: C-1 showing the MRT Values from July 15th to 18th

MRT Values: We can see the variation of values hereby in the table. The values increase in the early morning to reach peak value at 3 pm and start to decrease after that and reach lowest value in mid night.

Time	15th July -16th July (Degree C)	16th July-17th July) Degree C)	17th July-18th July (Degree C)
9 am	59.25	61.2	61.8
10 am	62.30	62.23	62.51
11 am	62	63.346	62.8
12 pm	64	65.77	65.9
1 pm	67	68.64	67.8
2 pm	70.15	70.31	70.6
3 pm	70.7	71.36	70.8
4 pm	66.8	67.77	67.5
5 pm	57.5	56.9	57.9
6 pm	31.87	31.90	32.6
7 pm	29.17	29.53	29.85
8 pm	28.23	27.69	27.62
9 pm	25.30	25.82	25.65
10 pm	22.52	25.21	24.45
11 pm	21.8	22.31	22.33
12 am	20.16	20.59	20.56
1 am	17.56	18.95	18.76
2 am	17.11	17.22	17.35
3 am	15.41	16.7	15.63
4 am	12.21	13.9	13.8889
5 am	32.38	33.11	33.247
6 am	46.96	46.8	47.98
7 am	53.24	55.5	58.35
8 am	59.5	60.12	58.2

Table C-2(For asphalt pavement region,15 July to 18th July 2022)

Direct Radiation

The following table shows Direct Radiation values from Envi-Met have been plotted. We can see the variation of values hereby in the table. The values increase in the early morning to reach peak value at 12pm

Time	15th July -16th July (W/m^2)	16th July-17th July(W/m^2)	17th July-18th July(W/m^2)
9 am	1014.82	1019.73	1019
10 am	1040.86	1043.27	1042.72
11 am	1052.74	1053.19	1052.69
12 pm	1052.78	1051.37	1050.88
1 pm	1040.98	1037.47	1036.97
2 pm	1014.93	1008.61	1008.04
3 pm	956.74	955.84	955.11
4 pm	848.39	847.53	846.37
5 pm	631.48	628.97	626.42
6 pm	21.34	9.87	51
7 pm	1	1	1
8 pm	1	1	1
9 pm	1	1	1
10 pm	1	1	1
11 pm	1	1	1
12 am	1	1	1
1 am	1	1	1
2 am	1	1	1
3 am	1	1	1
4 am	1	1	1
5 am	453.07	447	758.79
6 am	763.18	760.96	758.79
7 am	901	899.85	898.64
8 am	976.575	974.90	963.56

Table C-3 (For asphalt pavement region,15 July to 18th July 2022)

Reflected Radiation

The following table shows Reflected Radiation values have been plotted. We can see the variation of values hereby in the table. The values increase in the early morning to reach peak value at 12 pm

Time	15th July to 16th July W/m^2)	16th July to 17th July W/m^2)	17th July to 18th July W/m^2)
9 am	196.91	196.71	197
10 am	220	220	221.5
11 am	230.80	230.80	231
12 pm	228.647	228.5	229
1 pm	213.24	213.25	214
2 pm	186.24	186.3	186.5
3 pm	149.26	149.27	149.27
4 pm	163.99	162	162
5 pm	55	72	55.31
6 pm	1.067	.5922	2.703
7 pm	1	1	1
8 pm	1	1	1
9 pm	1	1	1
10 pm	1	1	1
11 pm	1	1	1
12 pm	1	1	1
1 am	1	1	1
2 am	1	1	1
3 am	1	1	1
4 am	1	1	1
5 am	25.46	25.05	25.45
6 am	73.05	72.63	73
7 am	120.27	119.88	120.21
8 am	162.53	162.19	163.21

Table C-4 (For asphalt pavement region,15 July to 18th July 2022)

Albedo Values (Found by dividing reflected radiation to direct radiation)

The following table shows Albedo values have been plotted. We can see the variation of values hereby in the table. The values increase in the early morning to reach peak value around 12 pm

Time	15th July -16th July	16th July-17th July	17th July-18th July
9 am	.183	.1871	.187
10 am	.203	.206	.205
11 am	.215	.214	.214
12 pm	.214	.214	.214.
1 pm	.205	.20	.20
2 pm	.18	.188	.18
3 pm	.153	.153	.182
4 pm	.120	.12034	.1521
5 pm	.08	.088	.083
6 pm	.34	.74	.13
7 pm	1	1	1
8 pm	1	1	1
9 pm	1	1	1
10 pm	1	1	1
11 pm	1	1	1
12 am	1	1	1
1 am	1	1	1
2 am	1	1	1
3 am	1	1	1
4 am	1	1	1
5 am	.0397	.038	.037
6 am	.085	.084	.083
7 am	.124	.1244	.123
8 am	.1588	.159	.153

Table C- 5 (For asphalt pavement region,15 July to 18th July 2022)

PET(Adult)

The following table shows PET values: have been plotted. We can see the variation of values hereby in the table. The values increase in the early morning to reach peak value around 6 pm

Time	15th July -16th July (Temp in Degree C)	16th July-17th July (Temp in Degree C)	17th July-18th July (Temp in Degree C)
9 am	21.4	21.6	21.7
10 am	26.5	26.8	26.9
11 am	31.3	31.4	31.6
12 pm	34	34.2	34.8
1 pm	36.1	36.2	36.4
2 pm	36.3	36.5	36.9
3 pm	38	38.2	38.5
4 pm	39	39.6	39.7
5 pm	39.2	39.4	39.7
6 pm	40.2	40.5	40.7
7 pm	38	38.6	38.8
8 pm	28	28.5	28.9
9 pm	28	28.6	28.9
10 pm	26.6	26.8	26.9
11 pm	21	21.5	22.1
12 am	21	21.7	22.2
1 am	25	25.9	26.2
2 am	20.6	20.8	21.4
3 am	19.3	19.4	20
4 am	18.2	18.4	19.2
5 am	16.2	16.4	17.2
6 am	21.2	21.4	22
7 am	17	17.2	17.7
8 am	16.9	17.2	17.6

Table C-6 (For asphalt pavement region,15 July to 18th July 2022)

PET(Child)

The following table shows PET values have been plotted. We can see the variation of values hereby in the table. The values increase in the early morning to reach peak value around 6 pm

Time	15th July -16th July (Temp in Degree C)	16th July-17th July (Temp in Degree C)	17th July-18th July (Temp in Degree C)
9 am	21.6	22.2	22.5
10 am	26.7	27.1	27.2
11 am	31.5	32	32.4
12 pm	34.5	34.8	35
1 pm	36.4	36.7	37
2 pm	36.7	36.9	37.2
3 pm	38.4	39.1	39.5
4 pm	39.4	40.1	40.2
5 pm	39.6	40	40.1
6 pm	40.54	40.52	40.6
7 pm	38.4	39	39.6
8 pm	28.5	28.8	29
9 pm	28.6	29	29.6
10 pm	26.8	27.2	28
11 pm	21.4	22	22.61
12 am	21.2	21.5	22.3
1 am	20.9	21.3	22.3
2 am	20.9	21.2	22.4
3 am	19.8	20.2	20.4
4 am	18.6	19.5	19.7
5 am	16.7	17.2	18.1
6 am	21.7	22	22.5
7 am	17.5	18.1	18.4
8 am	17.3	18.1	18.3

Table C-7 (For asphalt pavement region,15 July to 18th July 2022)

PMV (Adult)

The following table shows PMV values have been plotted. We can see the variation of values hereby in the table. The values increase in the early morning to reach peak value around 6 pm

Time	15th July -16th July	16th July-17th July	17th July-18th July
9 am	1.68	1.7	1.8
10 am	2.01	2.03	2.05
11 am	2.32	2.34	2.36
12 pm	2.50	2.52	2.54
1 pm	2.64	2.66	2,68
2 pm	2.65	2.67	2.69
3 pm	2.77	2.79	2.80
4 pm	2.83	2.85	2.86
5 pm	2.84	2.88	2.87
6 pm	2.91	2.93	2.95
7 pm	2.76	2.78	2.80
8 pm	2.11	2.13	2.15
9 pm	2.11	2.13	2.15
10 pm	2.02	2.04	2.06
11 pm	1.66	1.68	1.69
12 am	1.66	1.68	1.71
1 am	1.92	1.94	1.96
2 am	1.63	1.65	1.67
3 am	1.55	1.57	1.59
4 am	1.478	1.49	1.51
5 am	1.347	1.5	1.52
6 am	1.673	1.7	1.72
7 am	1.4	1.6	1.62
8 am	1.52	1.55	1.57

Table C-8 (For asphalt pavement region,15 July to 18th July 2022)

PMV (Child)

The following table shows PMV values have been plotted. We can see the variation of values hereby in the table. The values increase in the early morning to reach peak value around 6 pm

Time	15th July -16th July	16th July-17th July	17th July-18th July
9 am	1.7	1.73	1.74
10 am	2.04	2.06	2.07
11 am	2.34	2.37	2.39
12 pm	2.54	2.56	2.58
1 pm	2.67	2.69	2.71
2 pm	2.684	2.71	2.73
3 pm	2.79	2.82	2.84
4 pm	2.86	2.89	2.91
5 pm	2.87	2.89	2.91
6 pm	2.93	2.95	2.97
7 pm	2.80	2.82	2.84
8 pm	2.15	2.17	2.19
9 pm	2.155	2.172	2.19
10 pm	2.03	2.05	2.07
11 pm	1.68	1.71	1.73
12 am	1.67	1.68	1.70
1 am	1.654	1.68	1.70
2 am	1.654	1.68	1.70
3 am	1.58	1.60	1.62
4 am	1.50	1.52	1.54
5 am	1.38	1.42	1.44
6 am	1.70	1.72	1.74
7 am	1.43	1.45	1.47
8 am	1.42	1.45	1.47

Table C-9 (For asphalt pavement region,15 July to 18th July 2022)

Percentage of Satisfaction rate (Adult)

The following table shows Human Thermal Comfort (Adult) values have been plotted. We can see the variation of values hereby in the table. The values decrease in the after 9 am morning to reach a peak value around 6 pm and start to increase after that and reach the lowest highest value between midnight to early morning.

Time	15th July -16th July	16th July-17th July	17th July-18th July
9 am	35	34	33
10 am	26	24	22
11 am	20	19	17
12 pm	16	15	13
1 pm	14	13	12
2 pm	13	12	11
3 pm	11	10	9
4 pm	10	9	8
5 pm	10	9	8
6 pm	8	7	6
7 pm	11	10	9
8 pm	24	23	22
9 pm	24	23	22
10 pm	25	24	23
11 pm	32.3	31	30
12 am	32.3	31	30
1 am	27.3	26.5	25
2 am	33	32	30
3 am	36	34	32
4 am	36	34	32
5 am	36	34	32
6 am	36	35	33
7 am	35	35	33
8 am	35	35	33

Table C-9: Showing the Percentage of satisfaction rate of adult from 15th July to 18th July with 72-hour period(asphalt)

Table C-10 (For asphalt pavement region,15 July to 18th July 2022)

Percentage of Satisfaction rate (Child)

The following table shows Human Thermal Comfort (Child) values have been plotted. We can see the variation of values hereby in the table. The values decrease in after 9 am morning to reach a peak value around 6 pm and start to increase after that and reach the lowest highest value been midnight to early morning.

Time	15th July -16th July	16th July-17th July	17th July-18th July
9 am	32	31	30
10 am	25	24	23
11 am	19	18	17
12 pm	15	14	13
1 pm	13	14	13
2 pm	12	11	10
3 pm	10	9	8
4 pm	9	9	8
5 pm	9	8	7
6 pm	7	6	5
7 pm	10	9	8
8 pm	23	21	20
9 pm	23	22	20
10 pm	24	22	20
11 pm	31	30	29
12 am	31	30	29
1 am	26	25	24
2 am	32	31	30
3 am	34	31	30
4 am	34	33	32
5 am	34	33	32
6 am	34	33	32
7 am	33	32	31
8 am	33	32	31

Table C-10: Showing the Percentage of satisfaction rate of child from 15th July to 18th July with 72-hour period(asphalt)

Table D-1 Scenario D: (For concrete pavement region,15 July to 18th July 2022)

(Note:Table D-1 to Table D-10 are the output from Envimet

Table D-1

MRT Values: We can see the variation of values hereby in the table. The values increase in the early morning to reach peak value at 3 pm and start to decrease after that and reach lowest value in mid night

Time	15th July -16th July (Degree C)	16th July-17th July) Degree C)	17th July-18th July (Degree C)
9 am	59.25	61.2	61.8
10 am	62.30	62.23	62.51
11 am	62	63.346	62.8
12 pm	64	65.77	65.9
1 pm	67	68.64	67.8
2 pm	70.15	70.31	70.6
3 pm	70.7	71.36	70.8
4 pm	66.8	67.77	67.5
5 pm	57.5	56.9	57.9
6 pm	31.87	31.90	32.6
7 pm	29.17	29.53	29.85
8 pm	28.23	27.69	27.62
9 pm	25.30	25.82	25.65
10 pm	22.52	25.21	24.45
11 pm	21.8	22.31	22.33
12 am	20.16	20.59	20.56
1 am	17.56	18.95	18.76
2 am	17.11	17.22	17.35
3 am	15.41	16.7	15.63
4 am	12.21	13.9	13.8889
5 am	32.38	33.11	33.247
6 am	46.96	46.8	47.98
7 am	53.24	55.5	58.35
8 am	59.5	60.12	58.2

Table D-2 (For concrete pavement region,15 July to 18th July 2022)

Direct Radiation

The following table shows Direct Radiation values from Envi-Met have been plotted. We can see the variation of values hereby in the table. The values increase in the early morning to reach peak value at 12 pm

Time	15th July -16th July (W/m^2)	16th July-17th July(W/m^2)	17th July-18th July(W/m^2)
9 am	1014.82	1019.73	1019
10 am	1040.86	1043.27	1042.72
11 am	1052.74	1053.19	1052.69
12 pm	1052.78	1051.37	1050.88
1 pm	1040.98	1037.47	1036.97
2 pm	1014.93	1008.61	1008.04
3 pm	956.74	955.84	955.11
4 pm	848.39	847.53	846.37
5 pm	631.48	628.97	626.42
6 pm	21.34	9.87	51
7 pm	1	1	1
8 pm	1	1	1
9 pm	1	1	1
10 pm	1	1	1
11 pm	1	1	1
12 am	1	1	1
1 am	1	1	1
2 am	1	1	1
3 am	1	1	1
4 am	1	1	1
5 am	453.07	447	758.79
6 am	763.18	760.96	758.79
7 am	901	899.85	898.64
8 am	976.575	974.90	963.56

.

Table D-3 (For concrete pavement region,15 July to 18th July 2022)

Reflected Radiation The following table shows Reflected Radiation values have been plotted. We can see the variation of values hereby in the table. The values increase in the early morning to reach peak value at 12 pm

Time	15th July to 16th July W/m^2)	16th July to 17th July W/m^2)	17th July to 18th July W/m^2)
9 am	196.91	196.71	197
10 am	220	220	221.5
11 am	230.80	230.80	231
12 pm	228	228	229
1 pm	213.24	213.25	214
2 pm	186.24	186.3	186.5
3 pm	149.26	149.27	149.27
4 pm	163.99	162	162
5 pm	55	72	55.31
6 pm	1.067	.5922	2
7 pm	1	1	1
8 pm	1	1	1
9 pm	1	1	1
10 pm	1	1	1
11 pm	1	1	1
12 pm	1	1	1
1 am	1	1	1
2 am	1	1	1
3 am	1	1	1
4 am	1	1	1
5 am	25.46	25.05	25.45
6 am	73.05	72.63	73
7 am	120.27	119.88	120.21
8 am	162.53	162.19	163.21

Table D-4 (For concrete pavement region,15 July to 18th July 2022)

Albedo Values (Found by dividing reflected radiation to direct radiation)

The following table shows Albedo values have been plotted. We can see the variation of values hereby in the table. The values increase in the early morning to reach peak value around 12 pm

Time	15th July -16th July	16th July-17th July	17th July-18th July
9 am	.185	.1871	.186
10 am	.21	.26	.203
11 am	.214	.213	.216
12 pm	.217	.219	.218
1 pm	.203	.27	.22
2 pm	.185	.186	.14
3 pm	.149	.156	.180
4 pm	.124	.122	.1522
5 pm	.09	.0885	.082
6 pm	.36	.7	.2
7 pm	1	1	1
8 pm	1	1	1
9 pm	1	1	1
10 pm	1	1	1
11 pm	1	1	1
12 am	1	1	1
1 am	1	1	1
2 am	1	1	1
3 am	1	1	1
4 am	1	1	1
5 am	.0394	.0385	.037
6 am	.088	.085	.083
7 am	.122	.121	.123
8 am	.1589	.157	.153

Table D-5 (For concrete pavement region,15 July to 18th July 2022)

PET(Adult)

The following table shows PET values: have been plotted. We can see the variation of values hereby in the table. The values increase in the early morning to reach peak value around 6 pm

Time	15th July -16th July (Temp in Degree C)	16th July-17th July (Temp in Degree C)	17th July-18th July (Temp in Degree C)
9 am	22.4	22.6	21.6
10 am	27.5	26.9	26.3
11 am	32.3	31.4	30.8
12 pm	33	33.32	33.48
1 pm	38.2	37.21	35.45
2 pm	37.3	38.52	36.92
3 pm	37.5	38.86	38.52
4 pm	39.5	39.36	39.7
5 pm	39.3	39.52	39.96
6 pm	39.7	40.51	41.2
7 pm	37.8	39.61	38.4
8 pm	27.5	28.25	28.9
9 pm	27.8	27.62	27.5
10 pm	27.2	26.84	28.4
11 pm	27.5	23.5	21.1
12 am	21.3	22.7	24.2
1 am	25.4	21.94	25.4
2 am	20.2	20.4	20.4
3 am	19.2	19.64	18
4 am	17.9	18.34	18.2
5 am	16.8	15.9	16.2
6 am	18	20.3	20
7 am	17.3	17.5	16.5
8 am	18	17.7	17.8

\

Table D-6 (For concrete pavement region,15 July to 18th July 2022)

PET(Child)

The following table shows PET values have been plotted. We can see the variation of values hereby in the table. The values increase in the early morning to reach peak value around 6 pm

Time	15th July -16th July (Temp in Degree C)	16th July-17th July (Temp in Degree C)	17th July-18th July (Temp in Degree C)
9 am	21.8	22.32	22.3
10 am	26.8	27.21	27.5
11 am	31.3	33	32.6
12 pm	33.5	34.82	35.3
1 pm	35.4	35.78	36.4
2 pm	33.72	37.19	37.4
3 pm	37.43	39.12	39.6
4 pm	38.3	40.31	41.25
5 pm	39.16	39.6	40.3
6 pm	41.55	38.42	39.2
7 pm	37.46	39.2	38.4
8 pm	28.5	28.4	28
9 pm	28.62	28.6	27.3
10 pm	26.2	27.3	25
11 pm	22.4	22.1	21.61
12 am	24.2	21.2	20.3
1 am	21.9	21.5	19.3
2 am	18.9	21.6	18.43
3 am	18.83	20.1	17.4.4
4 am	18.6	19.3	19.7
5 am	16.47	17.1	16.13
6 am	22.7	21.8	20.55
7 am	18.15	22.3	22.4
8 am	17.3	18.1	18.3

Table D-7 (For concrete pavement region,15 July to 18th July 2022)

PMV (Child)

Time	15th July -16th July	16th July-17th July	17th July-18th July
9 am	1.63	1.68	1.79
10 am	2.00	2.01	2.01
11 am	2.3	2.32	2.33
12 pm	2.41	2.48	2.52
1 pm	2.6	2.62	2,64
2 pm	2.63	2.64	2.64
3 pm	2.72	2.75	2.78
4 pm	2.79	2.82	2.832
5 pm	2.76	2.84	2.82
6 pm	2.87	2.91	2.94
7 pm	2.82	2.72	2.82
8 pm	2.07	2.14	2.13
9 pm	2.1	2.11	2.14
10 pm	2.01	2.04	2.05
11 pm	1.66	1.62	1.66
12 am	1.66	1.63	1.70
1 am	1.94	1.95	1.92
2 am	1.62	1.61	1.63
3 am	1.53	1.56	1.52
4 am	1.472	1.42	1.48
5 am	1.343	1.54	1.47
6 am	1.675	1.68	1.69
7 am	1.36	1.58	1.61
8 am	1.51	1.53	1.52

Table D-8 (For concrete pavement region,15 July to 18th July 2022)

PMV (Adult)

The following table shows PMV values have been plotted. We can see the variation of values hereby in the table. The values increase in the early morning to reach peak value around 6 pm and start to decrease after that and reach the lowest value at midnight.

Time	15th July -16th July	16th July-17th July	17th July-18th July
9 am	1.6	1.65	1.72
10 am	2.37	2.03	2.01
11 am	2.31	2.3	2.29
12 pm	2.52	2.46	2.38
1 pm	2.62	2.58	2.68
2 pm	2.682	2.68	2.73
3 pm	2.73	2.78	2.85
4 pm	2.84	2.82	2.92
5 pm	2.87	2.86	2.98
6 pm	2.93	2.87	2.99
7 pm	2.82	2.79	2.82
8 pm	2.15	2.12	2.1
9 pm	2.055	2.052	2.02
10 pm	2.02	2.01	1.97
11 pm	1.64	1.68	1.84
12 am	1.62	1.64	1.76
1 am	1.61	1.62	1.70
2 am	1.59	1.61	1.67
3 am	1.52	1.59	1.62
4 am	1.49	1.52	1.54
5 am	1.38	1.42	1.43
6 am	1.38	1.40	1.42
7 am	1.42	1.41	1.6
8 am	1.48	1.45	1.63

Table D-9 (For concrete pavement region,15 July to 18th July 2022)

Percentage of Satisfaction rate (Adult)

The following table shows Human Thermal Comfort (Adult) values have been plotted. We can see the variation of values hereby in the table. The values decrease in the after 9 am morning to reach a peak value around 6 pm and start to increase after that and reach the lowest highest value between midnight to early morning.

Time	15th July -16th July	16th July-17th July	17th July-18th July
9 am	37	37	36
10 am	27	28	27
11 am	21	24	22
12 pm	16	17	16
1 pm	14	16	17
2 pm	13	15	13
3 pm	12	15	13
4 pm	11	14	11
5 pm	11	14	10
6 pm	9	13	9
7 pm	13	12	13
8 pm	26	15	25
9 pm	25	26	25
10 pm	26	28	26
11 pm	34.3	35	33
12 am	34.3	37	32
1 am	35	39	26
2 am	36	40	32
3 am	38	41	38
4 am	39	43	41
5 am	38	45	42
6 am	43	42	38
7 am	39	40	37
8 am	38	37	37

Table D-9: Showing the Percentage of satisfaction rate of adult from 15th July to 18th July with 72-hour period(concrete)

Table D-10 (For concrete pavement region,15 July to 18th July 2022)

Percentage of Satisfaction rate (Child)

The following table shows Human Thermal Comfort (Child) values have been plotted. We can see the variation of values hereby in the table. The values decrease in after 9 am morning to reach a peak value around 6 pm and start to increase after that and reach the lowest highest value been midnight to early morning.

Time	15th July -16th July	16th July-17th July	17th July-18th July
9 am	32	31	30
10 am	25	24	23
11 am	19	18	17
12 pm	15	14	13
1 pm	13	14	13
2 pm	12	11	10
3 pm	10	9	8
4 pm	9	9	8
5 pm	9	8	7
6 pm	7	6	5
7 pm	10	9	8
8 pm	23	21	20
9 pm	23	22	20
10 pm	24	22	20
11 pm	31	30	29
12 am	31	30	29
1 am	26	25	24
2 am	32	31	30
3 am	34	31	30
4 am	34	33	32
5 am	34	33	32
6 am	34	33	32
7 am	33	32	31
8 am	33	32	31

Table D-10: Showing the Percentage of satisfaction rate of child from 15th July to 18th July with 72-hour period(concrete)